



# Draft for discussion purposes

Report No. HR/TLG/2015-2016/1.3

## Estimation of lag time of water and nitrate flow through the Vadose Zone: Waikato and Waipa River Catchments

This report was commissioned by the Technical Leaders Group for the Healthy Rivers Wai Ora Project

The Technical Leaders Group approves the release of this report to Project Partners and the Collaborative Stakeholder Group for the Healthy Rivers Wai Ora Project.

Signed by:

**Date: 13 November 2015**

### Disclaimer

This technical report has been prepared for the use of Waikato Regional Council as a reference document and as such does not constitute Council's policy.

Council requests that if excerpts or inferences are drawn from this document for further use by individuals or organisations, due care should be taken to ensure that the appropriate context has been preserved, and is accurately reflected and referenced in any subsequent spoken or written communication.

While Waikato Regional Council has exercised all reasonable skill and care in controlling the contents of this report, Council accepts no liability in contract, tort or otherwise, for any loss, damage, injury or expense (whether direct, indirect or consequential) arising out of the provision of this information or its use by you or any other party.



## Draft for discussion purposes

# Estimation of lag time of water and nitrate flow through the Vadose Zone: Waikato and Waipa River Catchments

This report was commissioned by the Technical Leaders Group for the Healthy Rivers Wai Ora Project

The Technical Leaders Group approves the release of this report to Project Partners and the Collaborative Stakeholder Group for the Healthy Rivers Wai Ora Project.

Signed by:


**Date: 13 November 2015**

### Disclaimer

This technical report has been prepared for the use of Waikato Regional Council as a reference document and as such does not constitute Council's policy.

Council requests that if excerpts or inferences are drawn from this document for further use by individuals or organisations, due care should be taken to ensure that the appropriate context has been preserved, and is accurately reflected and referenced in any subsequent spoken or written communication.

While Waikato Regional Council has exercised all reasonable skill and care in controlling the contents of this report, Council accepts no liability in contract, tort or otherwise, for any loss, damage, injury or expense (whether direct, indirect or consequential) arising out of the provision of this information or its use by you or any other party.



**Estimation of lag time of water and nitrate  
flow through the Vadose Zone:  
Waikato and Waipa River Catchments**

**Report 1058-9-R1**

---

Scott Wilson & Ali Shokri

Lincoln Agritech Ltd  
15 September 2015

**MEASURE. MODEL. MANAGE.**

**Registered company office:**

Lincoln Agritech Limited

Engineering Drive, Lincoln University

Lincoln 7640

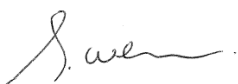
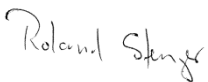

Christchurch

New Zealand

PO Box 69133

**Ph:** +64 3 325 3700

Document Acceptance:

| Action                                  | Name  | Date              |
|---|---|-------------------|
| Prepared and revised<br>by Scott Wilson |  | 15 September 2015 |
| Reviewed by Roland<br>Stenger           |  | 23 May 2015       |
| Approved for release<br>by Hugh Canard  |  | 25 May 2015       |

## EXECUTIVE SUMMARY

The travel time through the vadose zone can be an important component of the overall lag time between land use changes and associated surface water quality impacts. Therefore, this report presents a methodology and results for predicting the time taken for nitrate to travel from the land surface, through the unsaturated (vadose) zone and into shallow groundwater.

The modelling of vadose zone lag times in this report consists of three main stages; the calculation of land surface recharge with a soil moisture balance model, the calculation of vadose zone travel time, and the calculation of the time taken for the water and nitrate to penetrate into the uppermost aquifer layer. We collectively refer to the results of the vadose zone and saturated zone models as the total travel time. The input data for these calculations has been sourced from available climate, soil, geological, and hydrological databases. The results of all of our modelling are presented for the grid nodes and as sub-catchment averages (summary table in Appendix 1).

Mean annual rainfall varies from 1,126mm (Karapiro) to 2,338mm (Mangauika), and is generally highest in the western ranges from Te Pahu to Te Kuiti.

Mean annual land surface recharge tends to mirror rainfall in its distribution, and ranges from 136mm in the Waitawhiriwhiri sub-catchment to 909mm in the Mangauika sub-catchment (mean 365mm).

Recharge as a percentage of rainfall ranges from 11% in the Waitawhiriwhiri sub-catchment to 39% in the Mangauika sub-catchment (mean 25%).

The average vadose zone travel time was estimated to be shortest in the Waitomo catchment (6 years) and longest in the Torepatutahi catchment (77 years).

Our saturated zone calculations indicate that the time taken to penetrate the upper part of the aquifer ranges from 2.4 to 5.8 years (average 4.3), which is 10% to 40% (average 17%) of the total travel time.

Total travel times are less than ten years for most of the lower Waikato, Hamilton, and Waipa basins, particularly for elevations less than 100m. Short travel times are also found at higher elevations along the river and stream valley floors. This is particularly noticeable near Tokoroa and in the Reporoa Basin in spite of elevations of around 300m.

Longer travel times of 10 to 30 years are predicted for elevations above 100m, but are also predicted at some lower elevations along the catchment boundaries between streams.

The longest time lags are predicted beneath and in the vicinity of volcanoes and ranges, which is a function of a greater depth to the water table in these areas. However, there is greater uncertainty in predictions made in these areas, mainly due to the lack of information about the depth to the water table.

We have compared our model predictions with reported mean residence times for shallow tritium samples, and our model predictions agree well. The vadose zone model accounts for 75% of the variability in tritium mean residence times.

## TABLE OF CONTENTS

|  |           |
|--|-----------|
| <b>EXECUTIVE SUMMARY</b>               | <b>2</b>  |
| <b>LIST OF FIGURES</b>                 | <b>4</b>  |
| <b>LIST OF TABLES</b>                  | <b>5</b>  |
| <b>1 INTRODUCTION</b>                  | <b>6</b>  |
| 1.1 Study objectives                   | 6         |
| 1.2 Scope & nature of the services     | 8         |
| 1.3 Introduction to time lags          | 9         |
| 1.4 Conceptual model                   | 10        |
| <b>2 SOIL MOISTURE BALANCE MODEL</b>   | <b>12</b> |
| 2.1 Methodology                        | 12        |
| 2.2 Model inputs                       | 13        |
| 2.2.1 Soil data                        | 13        |
| 2.3 Model modifications                | 14        |
| 2.3.1 Runoff                           | 14        |
| 2.3.2 Readily available water          | 15        |
| 2.3.3 Interception                     | 15        |
| 2.4 Soil moisture balance results      | 16        |
| <b>3 UNSATURATED ZONE MODEL</b>        | <b>18</b> |
| 3.1 Theoretical background             | 18        |
| 3.2 Unsaturated zone methodology       | 19        |
| 3.2.1 Assumptions                      | 20        |
| 3.2.2 Numerical procedure              | 21        |
| 3.3 Vadose zone model parameterisation | 22        |
| 3.3.1 Static water levels              | 23        |
| 3.3.2 Hydraulic properties             | 27        |
| 3.4 Vadose zone model results          | 29        |
| <b>4 SATURATED ZONE MODEL</b>          | <b>32</b> |
| 4.1 Saturated zone model methodology   | 32        |
| 4.2 Total travel time results          | 33        |
| <b>5 COMPARISON WITH TRITIUM DATA</b>  | <b>38</b> |
| <b>6 REFERENCES</b>                    | <b>40</b> |

## LIST OF FIGURES

|  |    |
|--|----|
| Figure 1: Location map of the Healthy Rivers study area and the sub-catchments .....             | 7  |
| Figure 2: Conceptual hydrological setting for the time lag calculations.....                     | 10 |
| Figure 3: Land surface recharge (mm/year) as estimated by the soil moisture balance model .....  | 16 |
| Figure 4: Estimated land surface recharge as a percentage of mean annual rainfall .....          | 17 |
| Figure 5: Examples of water retention curves.....  | 18 |
| Figure 6 Vadose zone model parameter sensitivity analysis.....                                   | 23 |
| Figure 7: Interpolated static water levels for the study area showing the data sources .....     | 24 |
| Figure 8: Frequency distribution of static water levels in the Upper Waikato catchment .....     | 25 |
| Figure 9: Histogram of predicted depths to groundwater.....                                      | 26 |
| Figure 10: Map of interpolated depths to groundwater .....                                       | 27 |
| Figure 11: Predicted vadose zone travel times at each grid node.....                             | 29 |
| Figure 12: Predicted average vadose zone travel time for each sub-catchment.....                 | 31 |
| Figure 13: Conceptual model for saturated zone calculations.....                                 | 32 |
| Figure 14 Estimates of saturated travel time for one year's depth of land surface recharge ..... | 34 |
| Figure 15: Predicted total travel times at each grid node .....                                  | 35 |
| Figure 16: Predicted average total travel time for each sub-catchment .....                      | 37 |
| Figure 17: Comparison between predicted travel times and tritium mean residence time.....        | 39 |

## LIST OF TABLES

Table 1: SCS numbers, crop depletion factors, and interception values used for different land uses . 15

Table 2: Groundwater tritium data used for comparison with model predictions..... 38



# 1 INTRODUCTION

## 1.1 STUDY OBJECTIVES

Vertical flow through the unsaturated zone can account for a substantial fraction of the overall travel time from the root zone to a surface water body. Therefore, it is the objective of this study to calculate the time taken for nitrate to travel from the root zone of the soil to the water table (top of the saturated zone) in the Waikato and Waipa catchments.

We also estimate the time it takes for nitrate arriving at the water table to penetrate the uppermost saturated zone. The reason for this is that there are no opportunities to compare estimated travel times through the unsaturated zone with any existing independent data. However, a small number of mean residence time (MRT) estimates derived from sampling of shallow groundwater exist. Adding an estimate for the time it takes for an annual amount of land surface recharge to penetrate the saturated zone allows utilising the existing MRT estimates from groundwater sampled near the water table.

Our study forms a component of the Healthy Rivers-Wai Ora project, and the study area is shown in Figure 1.



**Figure 1: Location map of the Healthy Rivers study area and the sub-catchments**

Because of the regional nature of this project, a quite generalised approach had to be taken. The input data we have used is derived from regional-scale databases, and accordingly our calculations necessarily contain a number of simplifying assumptions. The results of our calculations are provided as area-weighted average values for each sub-catchment of the Healthy Rivers project, and as regional-scale maps of time lags. There are three main components to the project methodology:

1. Land surface recharge calculated by a daily soil moisture balance. This characterises drainage through the soil, and its variability across the region.
2. Estimating the vadose zone travel time. This estimation is based on soil drainage, depth to the water table, and the average calculated vadose zone water content
3. Estimating a nitrate mixing (or penetration) time for the upper, dynamic portion of the aquifer

The combination of these three components provides an average travel time from the land surface into shallow groundwater. The resulting data can be used produce maps of estimated time lags for nitrate accrual at the water table.

This report is divided into three main sections that cover the three main modelling components. The methodology, parameterisation, and results are covered within the section of each model component.

## 1.2 SCOPE & NATURE OF THE SERVICES

The scope of the study is specified in the project brief of 7 March 2014 and is as follows:

Estimate time of travel through unsaturated zones in the upper Waikato, Waipa and middle/lower Waikato River catchments. This will be achieved through the development of a contaminant lag time model incorporating both unsaturated zone and saturated mixing time for the study area.

A daily soil moisture balance for representative soils and lithologies will be estimated using appropriate methods to characterise drainage through the soil and its regional variability (Irrigation should be included where known).

Travel time through the unsaturated zone will be estimated based on soil drainage, depth to the water table and the estimated water content of the unsaturated zone.

An estimated mixing time for N (nitrate) in the upper parts of the aquifer through which shallow groundwater flow occurs (aquifer dynamic zone) will be included.

Validation of soil drainage estimates against known aquifer recharge estimates and validation of unsaturated zone travel times against available groundwater age data will be carried out.

Specific components comprise the following:

- An unsaturated zone soil moisture balance and lag model
- A saturated zone mixing time model
- GIS output of these models
- A report of resulting estimates including the methodology used in the development of the models and GIS output

It is acknowledged time lags associated with diffuse discharges comprise several other components: including the time for soil chemical properties to reach a new equilibrium following land use change and the time for the water resource to respond to the effect. These are not matters to be covered in this project.

### 1.3 INTRODUCTION TO TIME LAGS

The time lags associated with diffuse discharges consist of three main components (after Meals *et al.* 2010):

1. Time for a land-use change to have effect (social response)
2. Time for the effect to be delivered to the water resource (in this case shallow groundwater)
3. Time for the water body to respond to the effect (cumulative environmental impact)

The first of these components depends on changes in policy, and/or in land management. For example, the setting of limits for nitrate discharges could be written into a regional water plan, a process which would take some time. It may also take time for land managers to implement changes in their management practices. While these components cannot be easily estimated, they do need to be considered in the overall water quality response time.

This report deals specifically with the second of these time lag components. It assumes that a land-use change has occurred, and is starting to have an impact on soil water quality. This time lag can be considered as the:

*response time for an individual change in land use to be delivered to shallow groundwater*

This definition distinguishes an individual effect from a cumulative water body response at a specific location (e.g. monitoring well, spring discharge, or baseflow contribution to river).

In conceptual terms, the individual effect is characterised by a one-dimensional, gravity-driven vertical flow path from the soil into the top of the aquifer. By contrast, the cumulative water body response occurs in more of a horizontal direction along a groundwater flow path, and nitrate can be accrued with travel distance.

A distinction also needs to be made between groundwater pressure response and the actual flow of a molecule of water through the saturated or unsaturated zone. When a recharge event occurs, such as a high flow event in a river, there is an associated rapid groundwater response in the form of a pressure wave that travels across the aquifer. However, the individual water particles infiltrated during a recharge event will take considerably longer to travel through the unsaturated or saturated zones than the pressure wave. The reason for this is that particles need to negotiate the pore spaces of the sediment. Not all of the pore spaces will readily allow mobility, particularly around fine-grained sediments. For this reason, we use different analytical approaches to calculating pressure response times and contaminant transport response times.

The time for nitrate draining through the soil to be delivered to the water table depends on a number of factors including:

- Rate of drainage through the soil profile
- Depth to the water table
- Water content of the unsaturated zone
- Physical properties of the unsaturated zone
- Any biochemical attenuation processes that may occur

This study also includes an estimation of time taken to penetrate or mix in the uppermost, rainfall recharged portion of the aquifer.

## 1.4 CONCEPTUAL MODEL

The modelling of nitrate movement from the surface into shallow groundwater requires three main calculation steps:

1. Calculation of rainfall recharge (drainage through the soil profile)
2. Modelling the rate of flow through the unsaturated zone
3. A calculation to allow for time to mix in the shallow aquifer

These calculations are placed in a conceptual hydrological setting in Figure 2, where the circled numbers refer to the calculation steps listed above. The rainfall recharge calculation provides the input flow rate for both the unsaturated and saturated calculations. The unsaturated and saturated time-lag calculations are independent of each other, but when added together provide a total time lag estimate to the uppermost part of the aquifer.

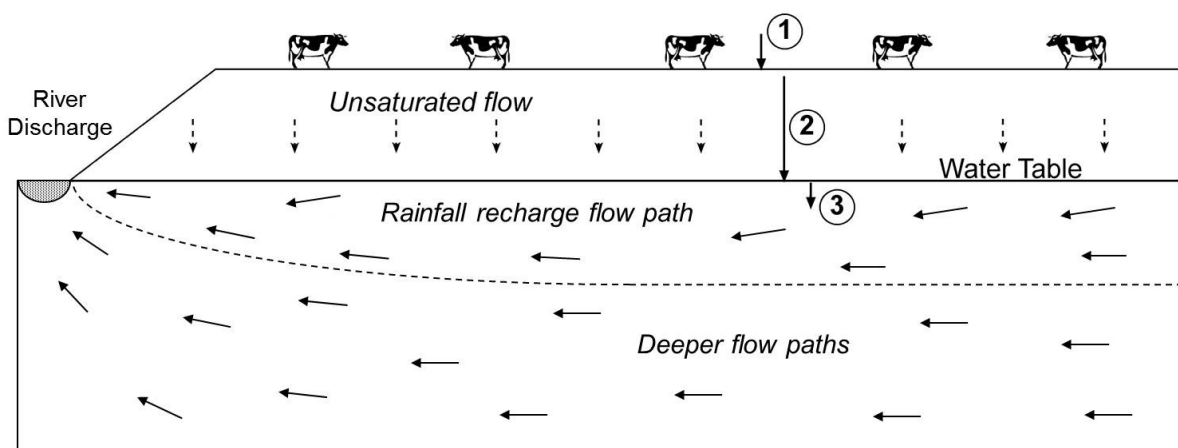


**Figure 2: Conceptual hydrological setting for the time lag calculations**

The calculations for the saturated zone are only carried out for a very thin part of the unconfined aquifer. The intention is to give an indication of the time it will take for leachate from the vadose zone to penetrate the uppermost groundwater zone. The reason for calculating this additional step is that

the groundwater zone is the point of interest in this study, since it is where the effect of nitrate leaching is observable and measureable. The calculation of vadose zone travel times alone is insufficient since it is practically extremely difficult to either sample, or interpret the impact of nitrate at the base of the vadose zone.

## 2 SOIL MOISTURE BALANCE MODEL

Land surface recharge was calculated using a daily soil moisture balance model, which has been modified from the Rushton model (Ruston *et al.* 2006, de Silva & Ruston 2007). This soil moisture balance model has proved to simulate lysimeter results quite accurately in New Zealand if the soil hydraulic properties are known (Wilson & Lu, 2011).

A key assumption made in the recharge calculations is that water is able to freely drain from the soil profile into underlying permeable geology. For groundwater recharge to occur there needs to be a suitable receiving medium underlying the soil profile. An assumption is also made that recharge is not intercepted by artificial drainage before reaching the water table.

### 2.1 METHODOLOGY

Spread-sheet calculations for soil moisture balance follow the algorithms provided in Rushton *et al.* (2006). The Rushton model consists of a two-stage process: calculation of near-surface storage and calculation of the moisture balance in the subsurface soil profile. The near-surface soil storage reservoir provides moisture to the soil profile once all the near-surface outputs have been accounted for. If there is no moisture deficit in the soil profile, recharge to groundwater occurs.

The Rushton model has been adapted for this report to incorporate run-off, which was calculated using the US Department of Agriculture, Soil Conservation Service (SCS) run-off curve number model. The SCS run-off model is described in Rawls *et al.* (1992).

There are three steps to describe the soil moisture balance:

1. Calculation of infiltration to the soil zone ( $I_n$ ), and near-surface soil storage for the end of the current day (SOILSTOR). Note that infiltration ( $I_n$ ), as specified by the Rushton algorithms, is not just infiltration (rainfall minus run-off), it also includes SOILSTOR from the previous day.
2. Estimation of actual evapotranspiration (AET). PET is derived by the Penman-Monteith equation (Allen *et al.* 1998), which uses short grass as reference crop. Most pastures in New Zealand behave like the reference crop for most of the year (Scotter & Heng, 2003). To account for differences between crops, different 'depletion factors' were used when calculating AET (Table 1).
3. Calculation of soil moisture deficit and groundwater recharge. Recharge occurs only when the soil moisture deficit is negative, i.e. when there is surplus water in the soil moisture reservoir.

The three steps outlined above partition near-surface soil storage between near-surface soil storage for the following day, AET, and the soil moisture deficit/reservoir respectively. The Rushton model is

usually started in winter when the initial soil moisture deficit can be safely assumed to be nil. This also allows a lead-in time for the model to give a satisfactory water balance for the following calendar year.

## 2.2 MODEL INPUTS

Rainfall and potential evapotranspiration (PET) data for the soil moisture balance model have been sourced from the NIWA virtual climate station database. This database consists of 473 climate sites across the study area with a grid spacing of approximately 5,550m x 4,400m.

The period of modelling that has been used to generate input data for the soil moisture balance model is 1 July 1983 to 31 Dec 2014. By starting the model in winter, we can assume that the initial soil moisture deficit is zero, and the model is given sufficient lead-in time to characterise soil conditions for the start on 1 January 1984. This produces a daily soil moisture balance model that covers a period of thirty years, sufficiently long to cover at least four El Niño-La Niña events.

### 2.2.1 SOIL DATA

In addition to rainfall and PET data, the soil moisture balance model requires input values for three soil hydraulic properties to calculate the daily water balance:

*Total Available Water (TAW)*. TAW is calculated from field capacity, wilting point and rooting depth data. Typical values for field capacity and wilting point are given in Table 19 of Allen *et al.* (1998), and many values for New Zealand soils can be found in the literature (e.g. McLaren & Cameron, 1996). It is more difficult to determine appropriate values for rooting depth. Values quoted in the literature are usually for uninhibited root penetration. Some knowledge of the soil profile is required to estimate rooting depth, because root penetration at a particular site may be limited by the presence of a resistive layer such as a loess or clay pan. If rooting depth is not known, it may be estimated from the profile thickness for thicker soil units. However, because rooting depth is also a function of water capacity and aeration properties of the soil, some caution is needed in using profile thickness as a proxy.

*Readily Available Water (RAW)*. RAW is related to TAW by a plant depletion factor,  $p$ . The depletion factor is the average fraction of TAW that can be depleted from the root zone before moisture stress sets in (reduction in transpiration). For NZ conditions,  $p$  should be around 0.4 to 0.6 for most plants, typically 0.5 for pasture<sup>1</sup>.

*Fracstor*. This is the near-surface soil retention. The contribution of Fracstor to the soil moisture balance is small, so errors resulting from estimations are considered to be negligible. Typical values are 0 for a coarse sandy soil, 0.4 for a sandy loam and 0.75 for a clay loam (Rushton *et al.* 2006, p. 388). Appropriate values can be estimated from field observations (de Silva and Rushton, 2007). If the soil dries quickly, then Fracstor will be less than 0.3. If the soil surface remains wet after heavy

---

<sup>1</sup> Coefficient values for a range of crop types may be found in Table 22 of Allen *et al.* (1998)



rainfall, so that it is not possible to work the soil for several days, then Fracstor is likely to be in the range 0.6–0.8.

For this study we have used the soil data provided by Landcare in the S-Map and Fundamental Soil Layer databases. S-map covers 50% of the study area, and we have used it in preference to the Fundamental Soil Layer database where coverage is available.

## 2.3 MODEL MODIFICATIONS

The simplest version of the soil moisture balance model we have used applies daily climate data to the soil reservoir with an additional calculation for runoff. Some modifications to the soil moisture balance model were considered necessary to include existing land use, canopy interception, and to account for land slope in the runoff calculations.

The spatial intersection of unique combinations of climate, soil, land use and slope input datasets produces a huge number of discrete soil moisture balance calculations. The final input dataset generated a total of 47,600 unique combinations of climate data, soil hydraulic properties, and land use. The model has been run for the full 12,540 day modelling period (>30 years) for each of these recharge zones. A Python script was written specifically to carry out the calculations in order to cope with the computational demand of such a large input dataset.

### 2.3.1 RUNOFF

The Rushton model has been adapted for this report to incorporate runoff (and interflow in steeper terrain), which is removed from the soil moisture balance. This was calculated using the US Department of Agriculture, Soil Conservation Service (SCS) runoff curve number model (SCS, 1972). The SCS runoff model is the most common method of runoff estimation (Ward & Elliot, 1995), and is best described in Rawls *et al.* (1992).

The SCS runoff method involves an attribution of a hydrological soil group for each soil (A to D). Soil group data for Waikato soils are available from the Landcare S-Map and Fundamental Soil Layer databases. A curve number is then estimated for each soil based on its hydrological soil group, which is used to calculate maximum soil retention for the calculation of runoff. Lower curve numbers give more water soil retention, and therefore less runoff. Pasture in good condition on free-draining soil has a low curve number, whereas pasture in poor condition on a poorly drained soil has a high curve number. A list of curve numbers for different soil conditions and land covers is given in Table 5.5.1 of Rawls *et al.* (1992), and the unadjusted values that we have used in our model are provided in Table 1.

The curve numbers shown in Table 1 have been adjusted within the soil moisture balance model to account for wet or dry antecedent conditions using the method of Ward and Elliot (1995). Adjustments have also been made for topography, since the SCS runoff method is assumed to be appropriate for slopes that are less than 5% (Williams, 1991). To account for the undulating terrain found throughout

the Waikato, as well as runoff in the steeper hill country, the curve numbers were adjusted by the method applied for the Erosion-Productivity Impact Calculator (EPIC), as documented by Sharpley and Williams (1990).

**Table 1: SCS numbers, crop depletion factors, and interception values used for each land use**

| CLUES<br>Landuse            | Land Area<br>(ha) | Land Area<br>(%) | SCS Number |    |    |    | Depletion<br>Factor | Interception<br>(mm) |
|-----------------------------|-------------------|------------------|------------|----|----|----|---------------------|----------------------|
|                             |                   |                  | A          | B  | C  | D  |                     |                      |
| Apples                      | 1,254             | 0.05             | 32         | 58 | 72 | 79 | 0.5                 | 1                    |
| Dairy                       | 512,199           | 21               | 49         | 69 | 79 | 84 | 0.6                 | 1                    |
| Deer                        | 238               | 0.01             | 39         | 61 | 74 | 80 | 0.6                 | 1                    |
| Grapes                      | 75                | 0.003            | 32         | 58 | 72 | 79 | 0.45                | 1                    |
| Kiwifruit                   | 1,158             | 0.05             | 32         | 58 | 72 | 79 | 0.35                | 1                    |
| Maize                       | 7,632             | 0.3              | 72         | 81 | 88 | 91 | 0.55                | 1                    |
| Native Forest               | 538,427           | 22.1             | 30         | 55 | 70 | 77 | 0.85                | 2                    |
| Onions                      | 6,351             | 0.3              | 72         | 81 | 88 | 91 | 0.3                 | 1                    |
| Other (wetlands, waterways) | 135,811           | 5.6              | 98         | 98 | 98 | 98 | 0.9                 | 1                    |
| Other Animals               | 2,685             | 0.1              | 39         | 61 | 74 | 80 | 0.6                 | 1                    |
| Plantation Forest           | 318,055           | 13               | 36         | 60 | 73 | 79 | 0.7                 | 2                    |
| Potatoes                    | 2,350             | 0.1              | 72         | 81 | 88 | 91 | 0.35                | 1                    |
| Sheep & Beef High           | 3,438             | 0.1              | 39         | 61 | 74 | 80 | 0.6                 | 1                    |
| Sheep & Beef Hill           | 325,342           | 13.3             | 68         | 79 | 86 | 89 | 0.6                 | 1                    |
| Sheep & Beef Intensive      | 384,366           | 15.7             | 49         | 69 | 79 | 84 | 0.6                 | 1                    |
| Scrub                       | 140,617           | 5.8              | 30         | 48 | 65 | 73 | 0.8                 | 2                    |
| Ungrazed Pasture            | 1,517             | 0.06             | 39         | 61 | 74 | 80 | 0.6                 | 1                    |
| Urban                       | 60,184            | 2.5              | 61         | 75 | 83 | 87 | 0.6                 | 1                    |

### 2.3.2 READILY AVAILABLE WATER

Values of RAW were derived by applying a representative soil water depletion factor to the TAW depending on predominant vegetation. FAO 56 (Allen *et al.* 1998) defines the depletion factor as the average fraction of TAW that can be depleted from the root zone before moisture stress occurs.

The land use data that has been used to assign appropriate depletion factors has been taken from the NIWA CLUES database for the Healthy Rivers project. Guideline values for different crop types are listed in FAO 56. A summary of values derived for other types of vegetation in temperate climates, for example coniferous and deciduous forest, is provided by Breuer *et al.* (2003). Table 1 lists the crop depletion factors that have been applied to the CLUES land uses based on these two reference sources.

### 2.3.3 INTERCEPTION

Canopy interception by different vegetation covers in New Zealand has been reviewed by Rowe *et al.* (2002). Their study found that canopy interception storage capacity tends to be on the order of 2mm for most types of woody vegetation reviewed. We have chosen to take a simple approach to account

for interception by removing for each event the first 1-2mm of rainfall in the soil moisture balance model. Canopy interception of 2mm was applied for scrub and forest (collectively 41% of the land area), and a value of 1mm was applied for all other land uses (Table 1).

## 2.4 SOIL MOISTURE BALANCE RESULTS

The results of the soil moisture balance model have been summarised as annual average values. The final model results are provided in (Figure 3) as recharge depths, and in (Figure 4) as a percentage of annual rainfall. Area-weighted averages for each sub-catchment are provided in Appendix 1.

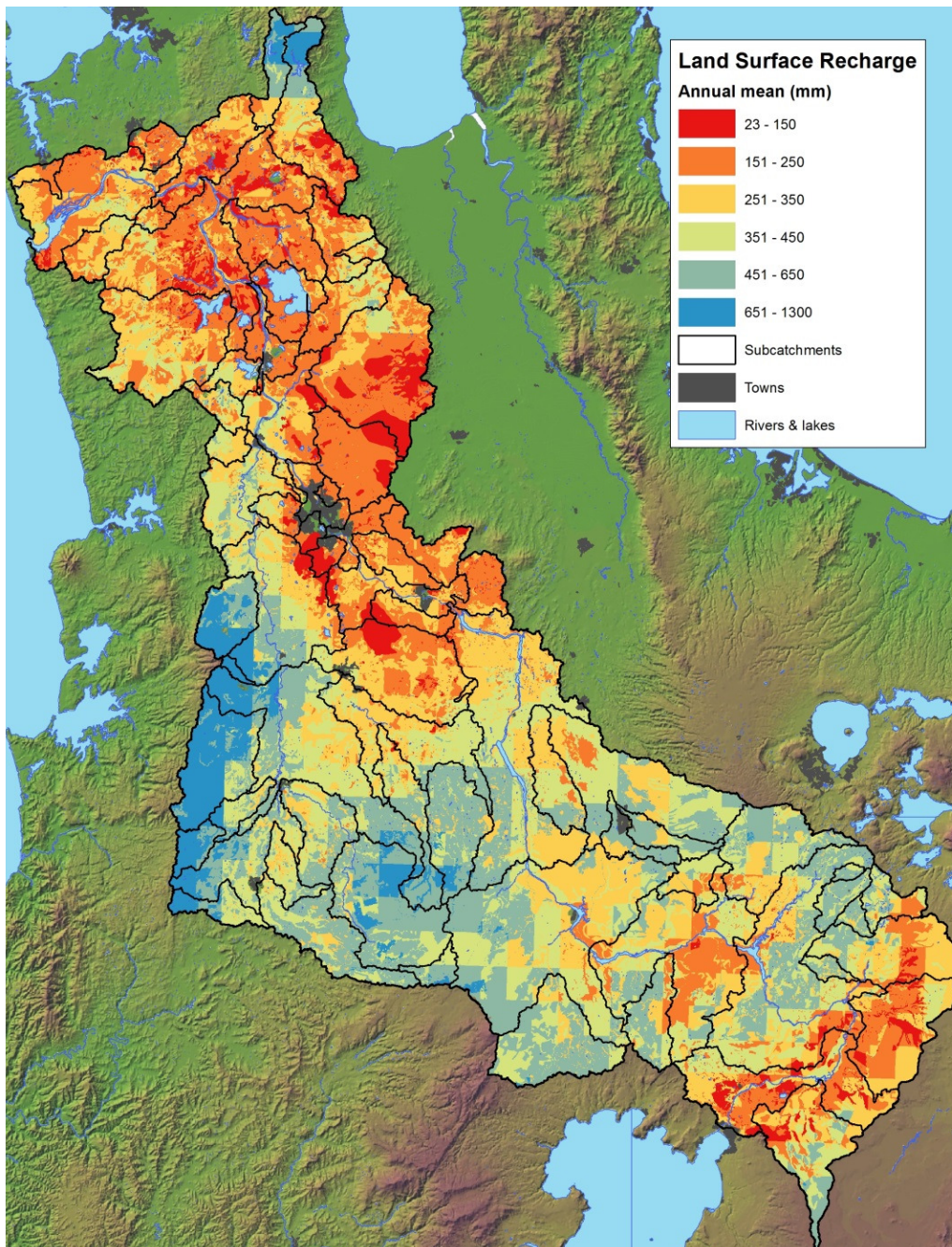


**Figure 3: Land surface recharge (mm/year) as estimated by the soil moisture balance model**

Some areas of Figure 3 show a blocky pattern in which the cells around the virtual climate stations are evident. This blocky pattern is caused by the spatial resolution of the climate station grid, which can't capture the rapid spatial increases in rainfall rate found in mountainous areas.

The evolution of our soil moisture balance modelling was iterative, as initial model runs gave unrealistic recharge percentage values. These values were iteratively reduced by adding runoff and interception components to the model. Some of the recharge percentages remain high (above 50%), although these are located in elevated areas with high rainfall rates and light soils.

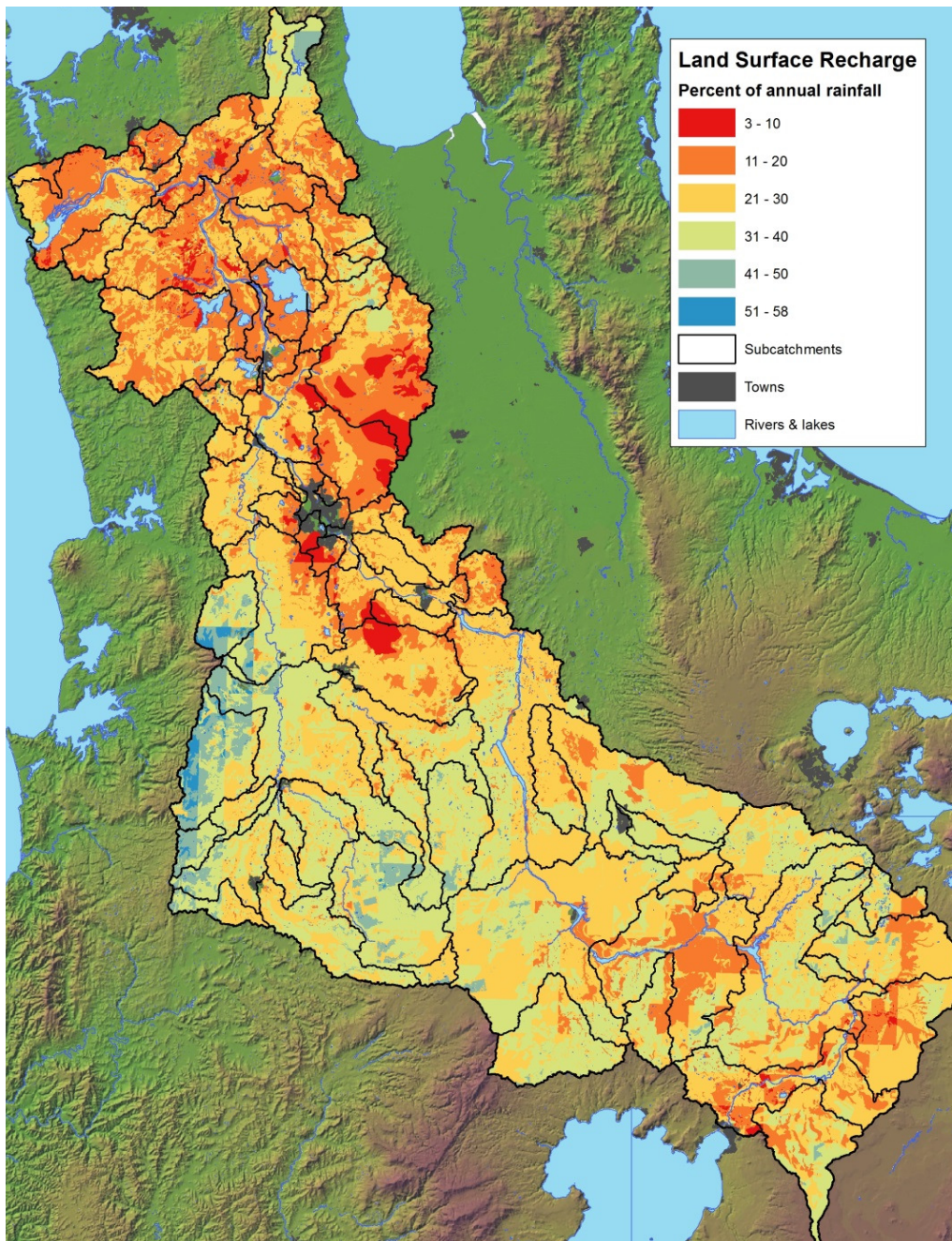


**Figure 4: Estimated land surface recharge as a percentage of mean annual rainfall**

### 3 UNSATURATED ZONE MODEL

Input parameters for the unsaturated zone model can be divided into three main components:

- Downwards flux (land surface recharge rates are derived from the soil moisture balance model)
- Travel distance (depth from the root zone to the water table)
- Hydraulic properties of the media (hydraulic conductivity, effective porosity, Van Genuchten parameters)

#### 3.1 THEORETICAL BACKGROUND

The greatest challenge to estimating travel time in the unsaturated (vadose) zone is the estimation of its average pore water content. Normally volumetric water contents are measured in the field using neutron probes, although such data is not available for the Waikato region. In the absence of measurements, this study makes use of reference water retention curves that have been developed for different sediment textures. These water retention curves describe the relationship between water content and capillary pressure for different sediments (Figure 5).

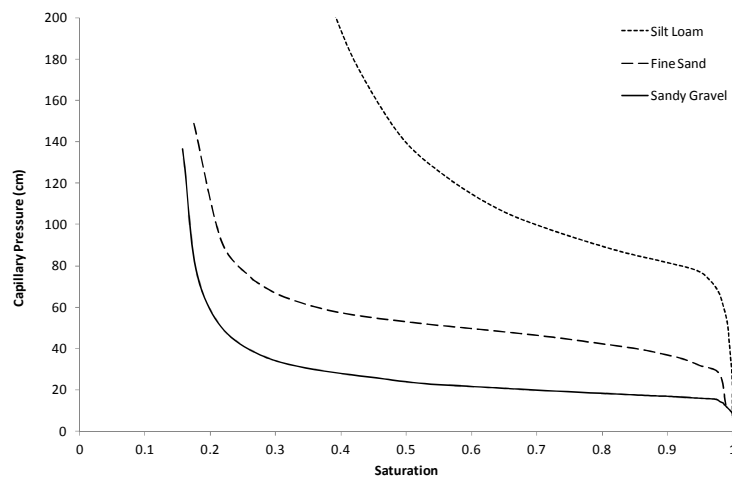


**Figure 5: Examples of water retention curves**

Because the vadose zone is semi-saturated, any inflow of water beneath the soil needs to overcome capillary tension in order for drainage to occur. Water retention curves allow us to characterise how readily water held under capillary pressure in the vadose zone will drain in response to land surface recharge. It can be seen in Figure 5 that the amount of water held in the vadose zone is largely determined by soil texture. The reason for this is that the hydraulic conductivity of the medium increases rapidly as the degree of saturation increases.

Sand and gravel drain quickly as capillary tension decreases compared to a silt or clay. This is because coarse sediments have a lot of large pore spaces with water that is only weakly held by capillary tension. This characteristic allows coarse sediments to recharge and drain quickly under

gravity. Conversely, silts and clays respond more slowly than sands and gravels, but their higher capillary tension enables them to stay saturated for longer. This means that the hydraulic conductivity of clay will be greater than that of gravel at low degrees of saturation, enabling the clay to continue to drain for a longer period of time.

The shape of water retention curves for different sediments has been modelled by a number of authors including Brooks and Corey (1964), Campbell (1974), Mualem (1976), and Van Genuchten (1980). For this report we have adopted the Van Genuchten method to characterise the shape of the soil-water retention curve. Unsaturated groundwater flow in porous medium is described by a 1D partial differential governing equation known as *Richards* equation.

The drainage velocity can be used to determine the average volumetric water content of the vadose zone:

$$\bar{\theta} = \frac{R}{v}$$

Where  $R$  is the land surface recharge flux, and  $v$  is the pore fluid velocity. The calculated water content is expressed either as a depth (volumetric water content ( $\theta$ ) in mm), or as a percentage saturation ( $S$ ). More permeable sediments tend to have lower volumetric water contents than fine grained sediments. Having estimated the average volumetric water content or saturation, the depth to the water table, and rate of soil drainage, we can then calculate the steady-state vadose zone travel time ( $t_{vz}$ ).

## 3.2 UNSATURATED ZONE METHODOLOGY

This section describes the methodology used to calculate the pore water content and travel time for the percolation of water through the unsaturated (vadose) zone.

There are many factors to consider for selecting the methodology and resolution of the modelling carried out. Ultimately it is the availability of data which defines the appropriate level of model sophistication and spatial resolution. Many of the factors important to detailed studies are not applicable at a regional scale. Dagan (1984) notes that a parameter that is critical at the site-scale (e.g. dispersion coefficient), becomes meaningless at the kilometre scale because of the uncertainties involved in characterising variability. The model applied also needs to match the available information. For example, *Sousa et al.* (2013) found that sophisticated and simplified methods gave similar results when the same knowledge of hydraulic conductivity was assumed.

The methodology used for this study has been developed with consideration that the investigation is of a regional nature. It calculates vertical travel times over an area of 1,102,300 hectares in a region that has negligible data on vadose zone properties. Accordingly, the model resolution chosen for this study is quite coarse, and our model grids are produced at a resolution of 500m<sup>2</sup> (25 hectares units).

### 3.2.1 ASSUMPTIONS

The approach to a regional-scale assessment needs to be pragmatic, requiring generalisation, and some judgement of which methodologies and parameters are most suitable for the scale of the subject matter.

With these considerations in mind, a number of assumptions have necessarily been made for this study:

- Drainage occurs in response to rainfall infiltration
- Flow is vertical (there are no flow barriers or artificial drainage)
- Flow is steady state
- Hydraulic properties at each site are homogeneous and isotropic
- The movement of nitrate is controlled by intergranular flow (between pore spaces)
- Nitrate behaves as a conservative solute (there is no sorption or denitrification)

Sorption (adherence) to particles can slow down the transport of solutes in the vadose zone. Close (2010) notes that nitrate does not tend to sorb within the vadose zone because nitrate and the medium it travels through are both negatively charged. Denitrification does occur within the soil horizon and can occur under certain conditions in the saturated zone. Denitrification is less likely to occur in the unsaturated zone below the soil zone because anoxic conditions are less common in that zone (e.g. Barkle *et al.*, 2014; Cannavo *et al.* 2002).

The assumption of vertical flow is not valid in areas of the Waikato where the water table is very shallow because these areas tend to be artificially drained. However, these areas are expected to have quite rapid vadose zone travel times even without artificial drainage (less than a year) because of their association with a shallow water table. Thus, the occurrence of artificial drainage doesn't significantly impact the results of our calculations, but it does limit the time resolution of our results to yearly estimates rather than monthly estimates.

The assumption of intergranular flow is most valid for unconsolidated lithologies where flow within the matrix pore spaces occurs, such as clastic sediments, tuffs and non-welded ignimbrites. If the substrate consists of volcanic flows, welded ignimbrites, or cemented sediments, there is a greater possibility of non-linear preferential (macropore or bypass) flow, which is very difficult to quantify. Non-linear flow can also occur as sediments approach saturation. The effect of saturation is to produce a large increase in the hydraulic conductivity of the sediments, which results in rapid flow through the larger pore spaces. As a result, faster vadose zone travel times could be a common occurrence in the wetter areas of the Waikato, particularly during winter and spring.

Vadose zone travel times are expected to be more rapid in areas of shallow water tables and higher recharge rates regardless of whether preferential flow occurs or not. Conversely, longer time lags are expected to occur primarily in areas where the water table is deep, but can also occur in drier areas, or where the substrate has a very low permeability.

It has been observed by Close (2010) that the centre of mass of tracer experiments in porous sediments does not vary as much as the rapid front or slower tail of the pulse. This allows us to derive a good first approximation of contaminant travel time for unconsolidated lithologies. However, in consolidated, harder lithologies, which are common in the Waikato region, preferential flow along fractures or joint planes can short circuit flow to the water table, particularly if the fractures or joints are vertically continuous over large depths. The influence of the macropores on vadose zone transport is very much dependent on fracture or joint density and geometry. Furthermore, preferential flow through joints and fractures normally occurs when there is ponded water or positive water pressure because substantial water flow into the macropores will only occur when fluid pressure exceeds the air entry pressure (Stephens, 1996).

The effect of preferential flow is to speed up the rapid front of a nitrate pulse. This quickens transport through the vadose zone so that root zone losses are transmitted to the water table more rapidly than can be predicted under the assumption of intergranular flow. While preferential flow certainly occurs throughout the harder lithologies in the Waikato, the bulk of the nitrate pulse may still lie within the slower tail of the pulse which moves through the lithology matrix via intergranular flow. The reason for this is the dependence that preferential flow has on macropore geometry and surface ponding.

Our vadose zone travel time calculations assume that the passage of water received from soil drainage moves to the aquifer by piston flow. This means that a volume of inflow from soil drainage displaces an equivalent volume from the vadose zone into the aquifer by a pressure response. The steady state travel time then becomes a function of the average volumetric water content of the vadose zone, effective porosity, and the depth to the water table:

$$t_{vz} = \frac{(S \cdot \phi \cdot l)}{R}$$

Where  $S$  is saturation (%), which can be derived from the Richards and Van Genuchten equations. The remaining parameters are either observed or estimated values, where  $l$  is depth to water table below the soil profile (m),  $\phi$  is effective porosity, and  $R$  is the soil drainage rate of land surface recharge (m/year).

### 3.2.2 NUMERICAL PROCEDURE

The approach for estimating travel time in the vadose zone with the Richards and Van Genuchten equations is described by Souza *et al.* (2013). The one-dimensional form of the Richards equation is used as a basis for estimating steady state flow through the vadose zone:

$$\frac{\partial}{\partial z} K(\psi) \frac{\partial h}{\partial z} = R$$

Where  $h$  is the pressure head,  $z$  is depth,  $K$  is the vertical hydraulic conductivity at variable saturation as a function of hydraulic head ( $\psi$ ), and  $R$  is the land surface recharge.

The Van Genuchten equations for characterising the shape of the soil-water retention curve are:



$$S(\psi) \begin{cases} S_r + \frac{1 - S_r}{[1 + \alpha \cdot \psi^\eta]^{(1-1/\eta)}} & \text{for } \psi < 0 \\ 1 & \text{for } \psi \geq 0 \end{cases}$$

$$K(\psi) = \begin{cases} K_s \cdot S_e^{0.5} \left[ 1 - \left( 1 - S_e^{1/(1-1/\eta)} \right)^{(1-1/\eta)} \right]^2 & \text{for } \psi < 0 \\ K_s & \text{for } \psi \geq 0 \end{cases}$$

Where  $S(\psi)$  is saturation as a function of pressure head,  $S_r$  is specific retention,  $K_s$  is saturated hydraulic conductivity,  $S_e$  is effective saturation  $(S-S_r)/(1-S_r)$ . Parameters  $\alpha$  and  $\eta$  are empirical coefficients related to the inverse air-entry pressure and pore-size distribution of the medium respectively. These two parameters are often referred to in literature as the Van Genuchten coefficients.

The numerical solution of the 1D Richards equation and the Van Genuchten equations yields pressure head, saturation and effective hydraulic conductivity. Having solved these, the travel time can be calculated as:

$$t = \int_0^l \frac{\varphi(z) \cdot S(z)}{R} dz$$

Where  $l$  is the thickness of the vadose zone (m),  $\varphi$  is effective porosity,  $S$  is the average volumetric water content, and  $R$  is land surface recharge or soil drainage (m/d).

### 3.3 VADOSE ZONE MODEL PARAMETERISATION

As a starting point for model parameterisation we estimated the range of parameter values expected for the study area and carried out a simple sensitivity analysis. The sensitivity of each parameter was determined by multiplying the input values by a factor and plotting the change in travel time estimations. The results, shown in Figure 6, indicate that depth to the water table and land surface recharge are the most sensitive parameters. The most sensitive hydraulic property was effective porosity. The hydraulic conductivity, Van Genuchten parameters and specific retention values were found to be relatively insensitive. The parameters are summarised in order of sensitivity as follows:

1. Depth to water table
2. Land surface recharge
3. Effective porosity
4. Hydraulic conductivity
5. Empirical Van Genuchten parameters and specific retention

We have therefore focussed our efforts on estimating the first three of these parameters as well as we can using the available data, particularly the depth to the water table.

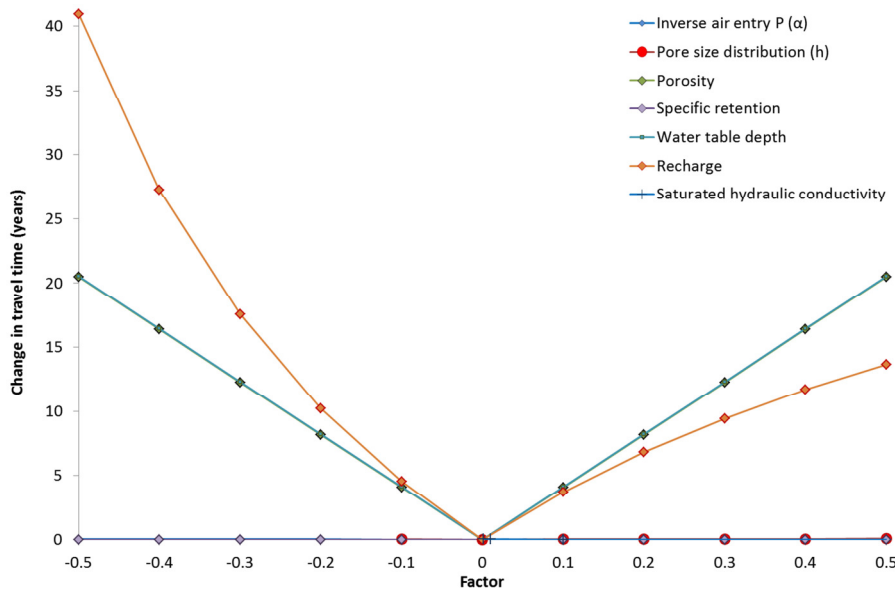


**Figure 6 Vadose zone model parameter sensitivity analysis**

### 3.3.1 STATIC WATER LEVELS

Vadose zone travel times are most strongly dependent on the distance travelled, which in this case is the depth from the root zone to the water table. Because of the sensitivity of calculations to the water table depth, it is important to estimate this parameter as accurately as possible.

Water table depths are available for 6,545 bores across the Waikato region, of which 4,115 are within the Healthy Rivers study area. Many of these sites are from deep bores that are not representative of the phreatic aquifer. To limit the dataset to shallow bores, the data were filtered to remove sites with casing depths greater than 30m and static water levels greater than 30m. This reduced the dataset to 3,365 sites, 2089 of which lie within the Healthy Rivers study area.

The Healthy Rivers study is concerned with sub-catchment totals or averages. This means we cannot simply calculate vadose travel times at points where we have groundwater depth observations. In order to determine the average vadose zone travel time with each sub-catchment, the static water levels are required to be interpolated across the region. In doing this interpolation, it becomes possible to calculate sub-catchment averages. We have accomplished this interpolation by fitting a variogram model to the observed water level dataset. The interpolated water level values were subsequently subtracted from the DEM to estimate the depth to groundwater on a 500m grid.

Initial interpolations gave large depths beneath hills, since there is very little groundwater information in these areas. The vadose zone model would thus give large travel times beneath hilly terrain, and give biased results in those sub-catchments. To try and improve the interpolation in hilly terrain, the borehole dataset was supplemented with estimates of surface water elevations for the River Environment Classification database (REC, Snelder *et al.* 2010) provided by Sandy Elliot of NIWA.

Low-order stream tributaries (1 and 2) were considered to be potentially ephemeral or perched and were removed from the dataset for variogram analysis.

The variogram analysis for the combined borehole level and REC dataset found that a spherical model with no nugget effect accounts for 99.9% of the observed covariance for distances less than 15km. The data were then kriged using the variogram structure to form a regional-scale static water level, which could then be subtracted from a DEM to create a depth to the water table at a 500m resolution. Figure 7 shows the resulting interpolated water table as well as the borehole and REC input data.

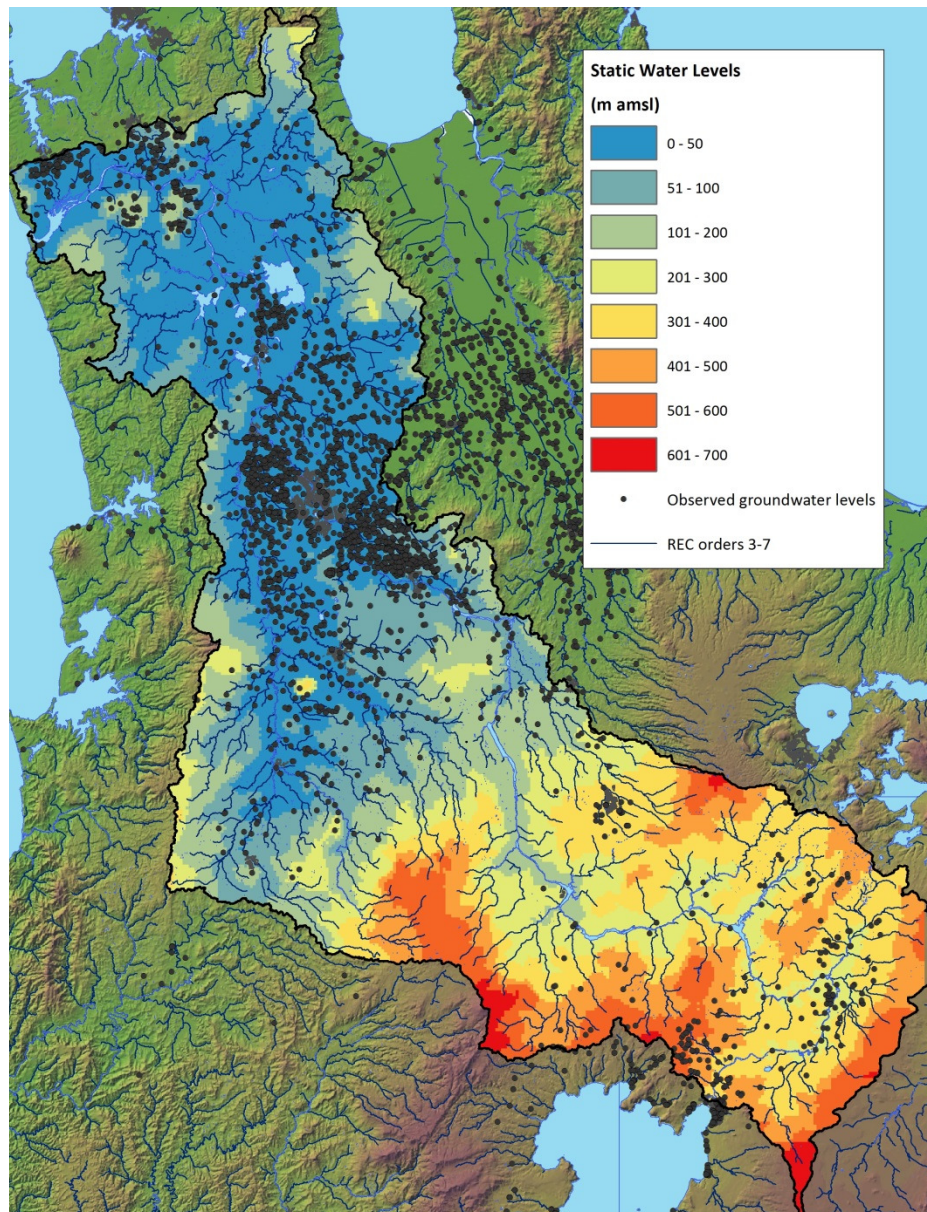


**Figure 7: Interpolated static water levels for the study area showing the data sources**

The water table produced by the Upper Waikato groundwater model (Weir & Moore 2011) was initially used as a data source for the interpolation. Data for the top layer of the Stage 5 model were supplied courtesy of Julian Weir (Aqualinc), and included in the variogram analysis. The results did not produce

models with as good a fit as those produced by the groundwater level and REC data alone. The reason for this is almost certainly the 1km groundwater model grid, which is a coarse resolution compared to the groundwater and REC observations, which could be contoured at 500m resolution.

Figure 8 shows a histogram of static water levels to illustrate the comparison between different data sources over the domain of the Upper Waikato groundwater model. The three datasets shown are the interpolated dataset produced by our study, groundwater level observations, and values predicted by the Upper Waikato groundwater model. The groundwater model is slightly better at predicting water levels at higher altitudes, although these values account for less than 0.5% of the model dataset.

There are two main limitations that we have encountered with the available datasets. The first is the availability of data in steeply sloping areas. These data are not available for training of the variogram model, and hence are not captured by the interpolation. The resulting interpolated water table surface is considerably more gently sloping (more subdued) than the land surface in the study area. This can produce groundwater levels above the land surface in steeply sloping areas (e.g. the flanks of volcanoes).

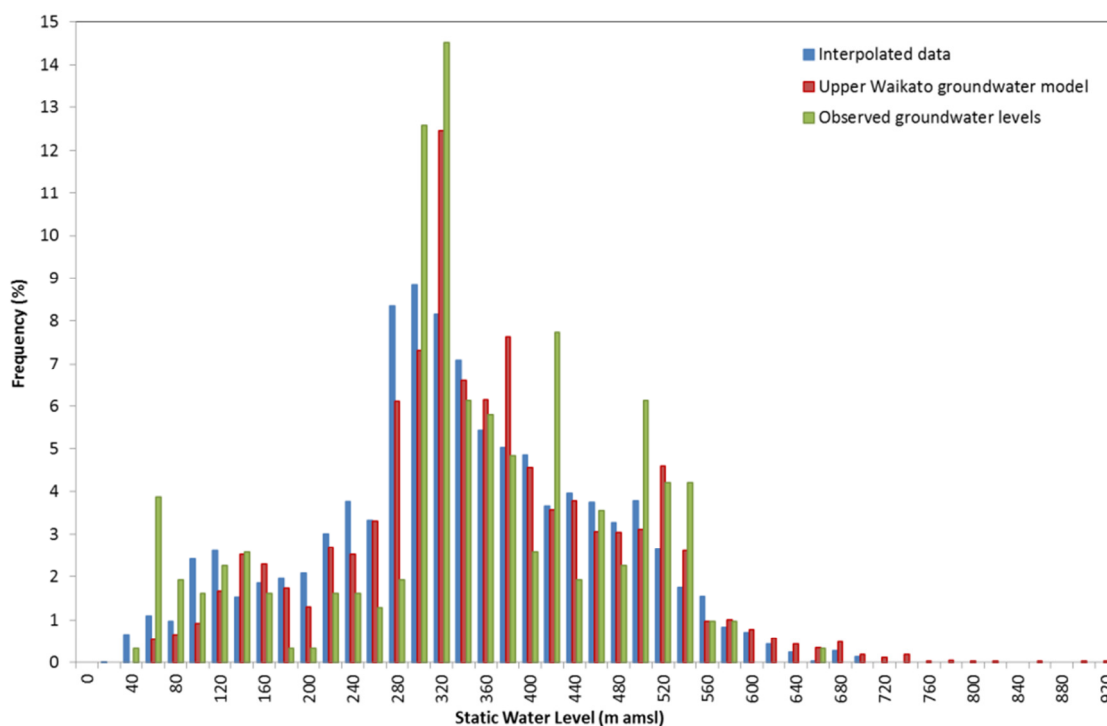


**Figure 8: Frequency distribution of static water levels in the Upper Waikato catchment<sup>2</sup>**

The second limitation is the availability of data points at higher elevations for interpolating. The absence of these control points results in a water table interpolation which projects underneath hills rather than rising with the topography. To some extent we have tried to overcome this by the inclusion of the mid-order REC elevations. Despite our efforts there are regions of the study area where the

<sup>2</sup> Histogram bins are '0' for 0-9m, '10' for 10-19m etc.

interpolation has predicted unrealistically deep water tables (e.g. Hunua Range, Pirongia, Maungatautari, Rangitoto Range).

An expansion of the dataset to include bore depths and static water levels greater than 30m adds more 33 sites for kriging, although only 6 of these have recorded bore depths. These additional sites do not significantly improve our water table elevation estimates because bores do not tend to be drilled on mountainsides.

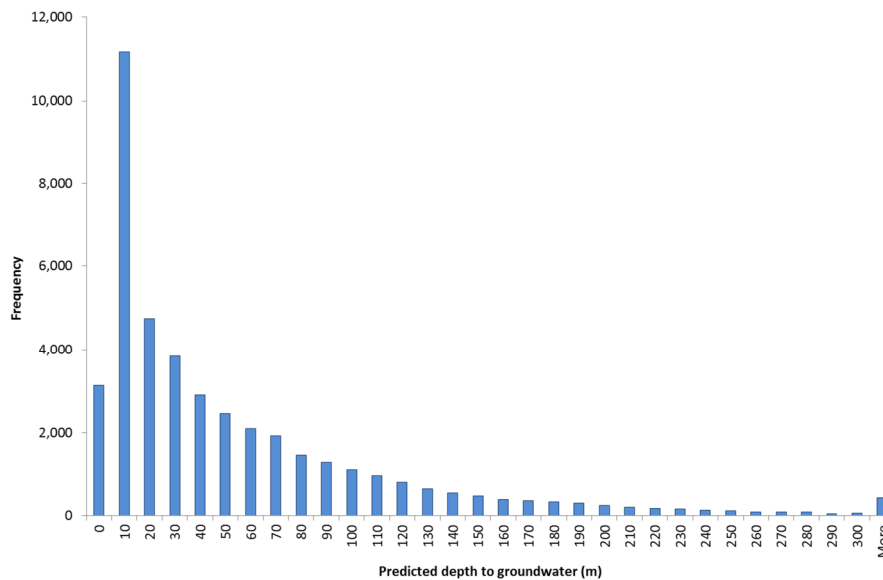


**Figure 9: Histogram of predicted depths to groundwater**

The interpolated deep water tables create a problem for our vadose zone model calculations. To include deep water tables in our dataset would introduce a large bias in our average sub-catchment travel time calculations. We therefore need to select a threshold value and remove water table depths that are considered unrealistically deep. Figure 9 shows a histogram of the water table depths that have been predicted for the entire 500m x 500m grid.

Unfortunately there are no breaks in the slope of the histogram at higher elevations that we could use to identify a threshold. With the absence of any observational data to guide us, we have chosen to select a value that captures 90% of the dataset. This means that we have deleted all interpolated depths that are greater than 130m depth. The final map of groundwater depths is shown in Figure 10.

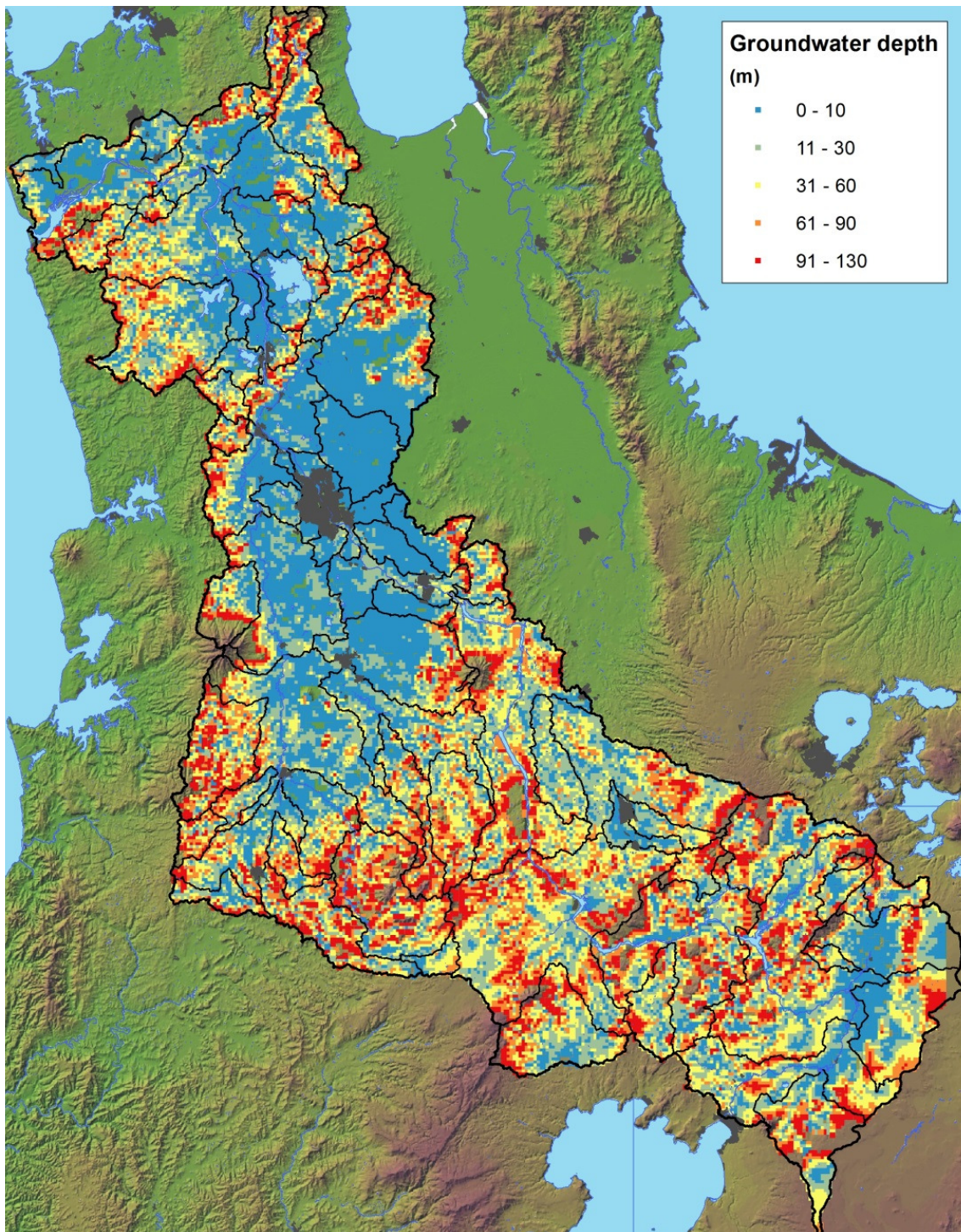


**Figure 10: Map of interpolated depths to groundwater**

### 3.3.2 HYDRAULIC PROPERTIES

In addition to recharge depth and depth to groundwater, we also need to estimate the physical characteristics of the medium. The only parameter values available for the vadose in the region come from the Spydia study within the Taupo Ignimbrite (Wöhling *et al.* 2008). We have therefore used a range of reported values for Waikato groundwater, as well as estimates from other studies worldwide to parametrise the vadose zone model.

The baseline dataset for the distribution of lithologies was the GNS QMap series (Edbrooke 2001 & 2005, Leonard et al 2010). QMap maps the distribution of surface geology, and an assumption is made in this report that the surface geology is representative of the rocks situated between the surface and the water table. The characteristics in Qmap that enable hydraulic properties to be parametrised are the main rock, stratigraphic age (an indicator of induration or cementation), and the stratigraphic description of each unit.

The most insensitive parameter, specific retention is assumed to be 5% for all stratigraphic units. Values for the Van Genuchten parameters  $\alpha$  and  $\eta$  were taken from Wöhling *et al.* (2008) for the Taupo ignimbrite. Typical values for tuffs were taken from Flint (2003) who reported values for a large range of samples from the Yucca Mountains. Values for clastic sediments were attributed values reported by Shaap et al. (1999). To expand the dataset we have derived equivalent textures of clastic sediments for the volcanic lithologies. This was done by comparing typical grain sizes as outlined by the NZ Geotechnical Society (2005), for example a fresh ignimbrite has an equivalent texture of silty clay.

Appendix 2 lists the lithologies found within the study area, their textures, hardness, and appropriate parameter values derived from textural equivalence. Some variation was given to the texture assigned according to the hardness in the lithological description. Softer lithologies have been downgraded a texture, and firm lithologies have been upgraded a texture. Some lithologies are described as hard, and we have assumed these are either volcanic flows, or cemented sediments. These lithologies have been assigned a clayey form of the primary texture.

Because of their higher sensitivity in our vadose zone model, porosity values were further refined from those provided by the textural equivalence exercise. Values for hydrothermally altered rocks of the Taupo Volcanic Zone are reported in Wyering *et al.* (2014), and values for the dominant units in the Upper Waikato catchment were provided by GNS Science for Weir and Moore (2011). Representative porosity values are reported for a variety of clastic sediment and volcanic lithologies in McWorter and Sunada (1977), Freeze and Cherry (1979), Domenico and Schwartz (1998), and Singhal and Gupta (2010).

Hydraulic conductivity values are the most sensitive of the hydraulic parameters, and we have tried to source values that are characteristic of individual geological units rather than simply allocating values to each lithology. Where aquifer test data were available in the WRC database we have used those values by preference. Many of these test results are summarised for the Upper Waikato catchment in Tschritter *et al.* (2014). While the aquifer test values may be influenced by secondary porosity (fracture flow), we have assumed that the reported results are from late-time test data. Aquifer tests in dual-porosity systems are normally continued until the primary porosity response is apparent since it is expected to be more representative of long term bore yield. Hydraulic conductivity values for units other than those covered by the preceding sources were derived from a GNS dataset that was produced for the Healthy Rivers project.

### 3.4 VADOSE ZONE MODEL RESULTS

The results of our vadose zone travel time calculations at each 500m grid node are shown in Figure 11. Some of the grid nodes have given unrealistically large travel times (>100 years). These sites have tended to have extremely low unsaturated flow velocities. When the velocity is less than the recharge rate, recharge is expected to be refused by the substrate beneath the soil profile, and ponding, interflow or runoff will occur. To account for this, we have removed vadose zone model results with vertical velocities less than 10cm/year.

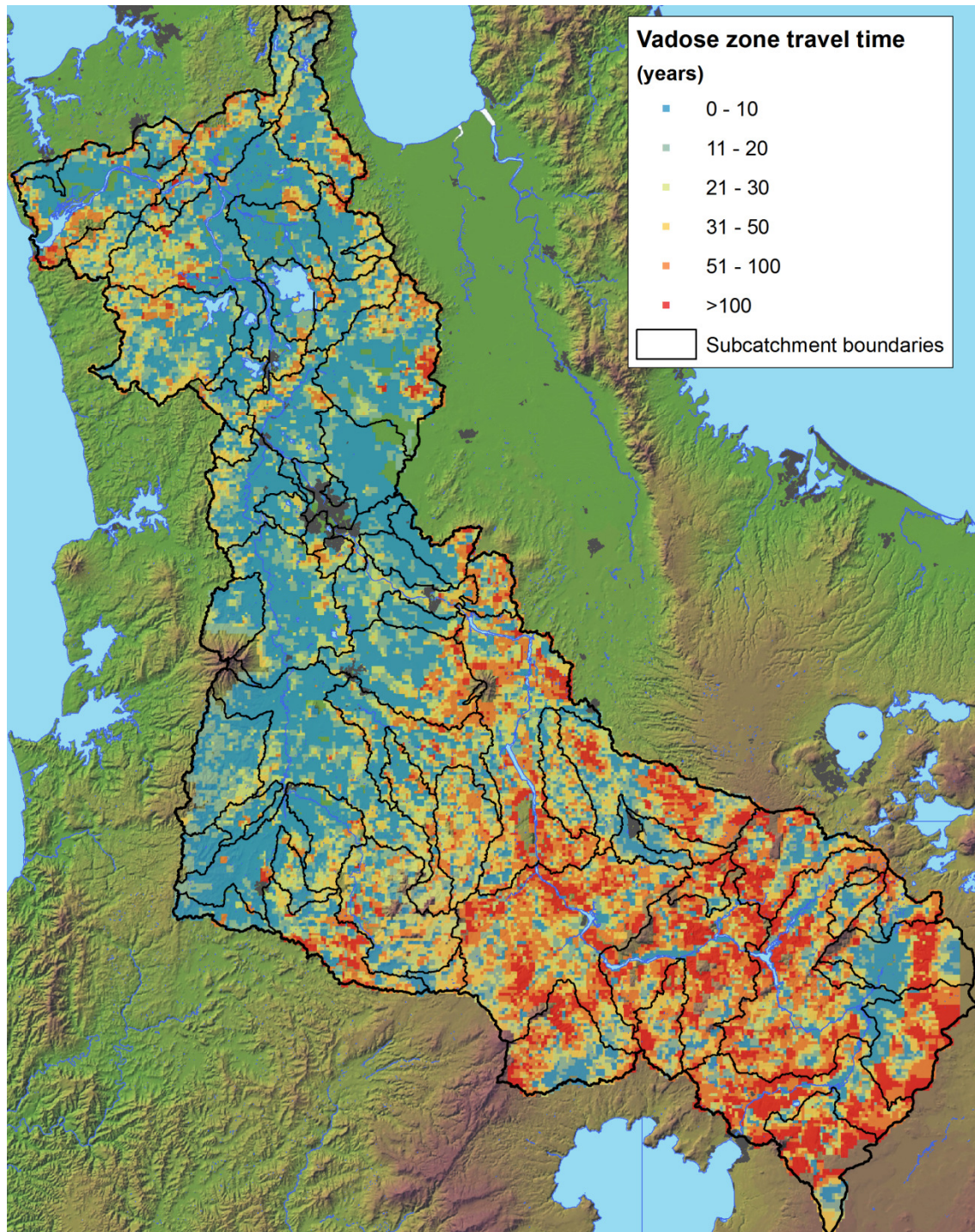


Figure 11: Predicted vadose zone travel times at each grid node



The spatial distribution of our predictions shows the overwhelming influence that the depth to the water table has on our results. Most of the greater lag times are located along ridgelines and in the Upper Waikato and Upper Waipa catchments where the water table is deeper. Most sites at lower elevations within the study area (<100m amsl) are predicted to have vadose zone travel times of less than 10 years.

Figure 12 shows the predicted average travel time for each sub-catchment, and the results are also listed in Appendix 1. The sub-catchment vadose zone lag times are predicted to range from 6.4 to 76.7 years with an average of 27.3 years.

The sub-catchment averages have been determined by calculating a weighted average of the travel time values calculated at the grid nodes. The weighting was based on the land surface recharge flux, which represents the amount of water flowing vertically through each cell in the model. The rationale for this is that the contribution of each model cell to the sub-catchment discharge depends on its relative contribution to the total flow, regardless of the thickness of the vadose zone.

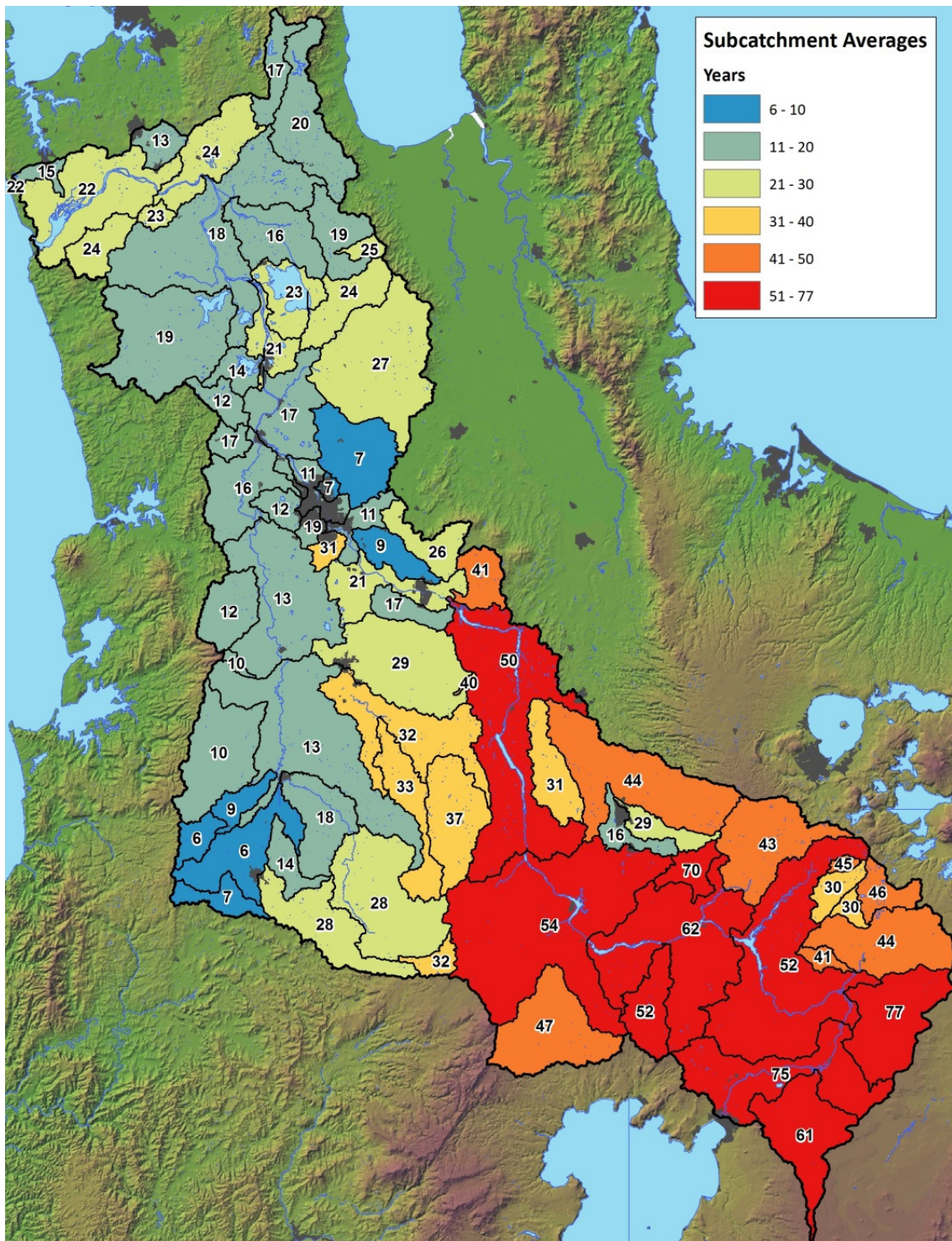


**Figure 12: Predicted average vadose zone travel time for each sub-catchment**

When interpreting the results of our model as displayed in map form (Figure 11), it is important to consider that our lag times refer to the vertical flow path from the land surface into the water table. It is therefore not appropriate to relate our predictions to the results of tritium mean residence times from stream samples. This is because water that enters a stream on shallow flow paths (e.g. runoff or interflow) is considerably younger than that from groundwater pathways.

## 4 SATURATED ZONE MODEL

This section of the report describes a method for calculating the time taken for nitrate from the vadose zone to penetrate the upper most dynamic part of the shallow aquifer. Vertical movement through groundwater tends to be relatively slower than movement through the vadose zone.

The reason for accounting for nitrate penetration into the saturated zone is that this is the zone where nitrate input from the vadose zone will have an observable and measurable effect, for example in water supply bores. Also, the base of the vadose zone is difficult to sample for practical reasons. By accounting for penetration into the saturated zone we can compare our travel-time estimates with mean residence times estimated from tritium analysed in groundwater samples taken from the uppermost saturated zone.

### 4.1 SATURATED ZONE MODEL METHODOLOGY

To describe penetration of nitrate into the uppermost groundwater zone, a mixing depth equivalent to a year of annual rainfall recharge has been selected. This mixing depth has been calculated by dividing the mean annual rainfall recharge by the effective porosity for each site. This depth is equivalent to  $1\text{m} \pm 0.5\text{m}$  for the majority of sites used in this study. It is expected that groundwater in this shallow depth range will be entirely recharged from the land surface above. Exceptions to this rule will apply in close proximity to streams.

Figure 13 shows the conceptual model for the saturated zone modelling undertaken for this study. For a homogenous unconfined aquifer with uniform land surface recharge and the boundary conditions presented in Figure 13, groundwater at a specific depth ( $t_1, t_2, \dots$ ) is all equal in age (Appelo & Postma, 2005). This simple conceptual model allows us to easily make analytical calculations for nitrate penetration into shallow groundwater and enables us to estimate the total travel time from the soil to the upper aquifer at a regional scale.

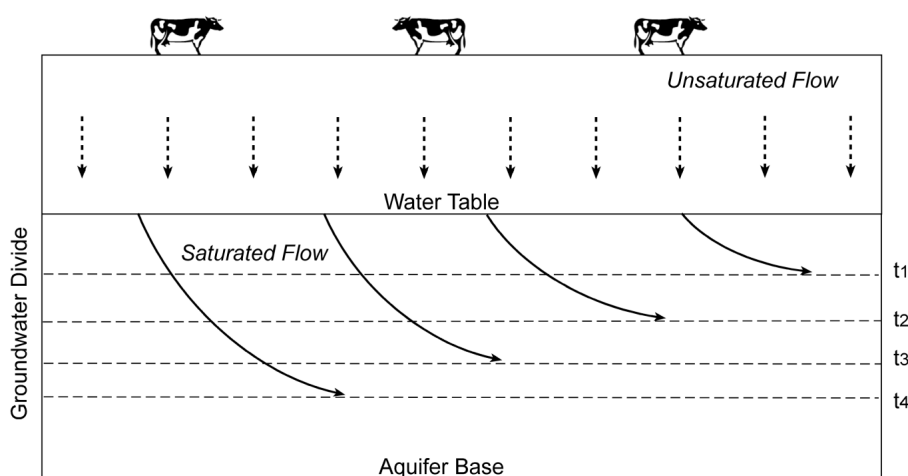


**Figure 13: Conceptual model for saturated zone calculations**

The boundary condition requirements for Figure 3 can be satisfied if the model is positioned within a regional setting at a shallow level (shown in Figure 1). The groundwater divide for the rainfall recharge pathway can be set at the river. The base of the aquifer can effectively be set where the flow lines are close to horizontal. These boundary configurations imply that a simple model will give a good estimate of vertical groundwater travel time for shallow depths. However, a simple model won't provide reliable results in the vicinity of river recharge and discharge areas. This is because groundwater flow paths in these areas diverge and converge respectively and deviate markedly from the horizontal.

A simple analytical model will now be presented that is based on the boundary conditions shown in Figure 3. Vertical flow through the uppermost portion of an unconfined aquifer that is recharged from the land surface can be approximated by the following equation:

$$t_{sat} = \ln\left(\frac{D}{D-d}\right) \frac{D\varphi}{R}$$

Where  $D$  is aquifer saturated thickness,  $d$  is depth below water table (m),  $R$  is land surface recharge (m/year), and  $\varphi$  is effective porosity (Appelo & Postma, 2005). As described above, the mixing depth  $d$  has been calculated as one year of land surface recharge divided by the porosity. At the time of writing, no information was available for aquifer saturated thickness. This information is expected to be available in the near future when the results of the Healthy Rivers GNS geological model become available. Until then, we have used an interim uniform saturated depth of 100m. Other parameter values used for our calculations are the same as those used for the unsaturated zone calculations.

For this estimation the aquifer is assumed to be homogeneous, and horizontal flow velocity is equal with depth. These assumptions can be considered to be reasonable for the purposes of providing regional estimates of time lags that include nitrate penetration into the aquifer. The reason for this is that at a regional scale, most aquifers have horizontal dimensions that are far greater than the vertical (kilometres compared to metres).

However, the horizontal flow assumption is not valid in the vicinity of surface water bodies. If we looked at a profile through an aquifer that is recharged by river losses, we would see groundwater flow lines diverging away from the river. Conversely, we would see flow lines converge as they approach an area where a groundwater contribution to river baseflow occurs. For this reason, our saturated mixing time calculations are not valid in the vicinity of surface water bodies. Calculations in these areas can be made with more complex 2D or 3D flow equations.

## 4.2 TOTAL TRAVEL TIME RESULTS

The predicted saturated time component of the total travel time ranges from 2.4 to 5.8 years (average 4.3), which is 10% to 40% (average 17%) of the total travel time. A map of the calculated saturated travel time for one year's annual recharge at each 500m grid node are shown in Figure 14.

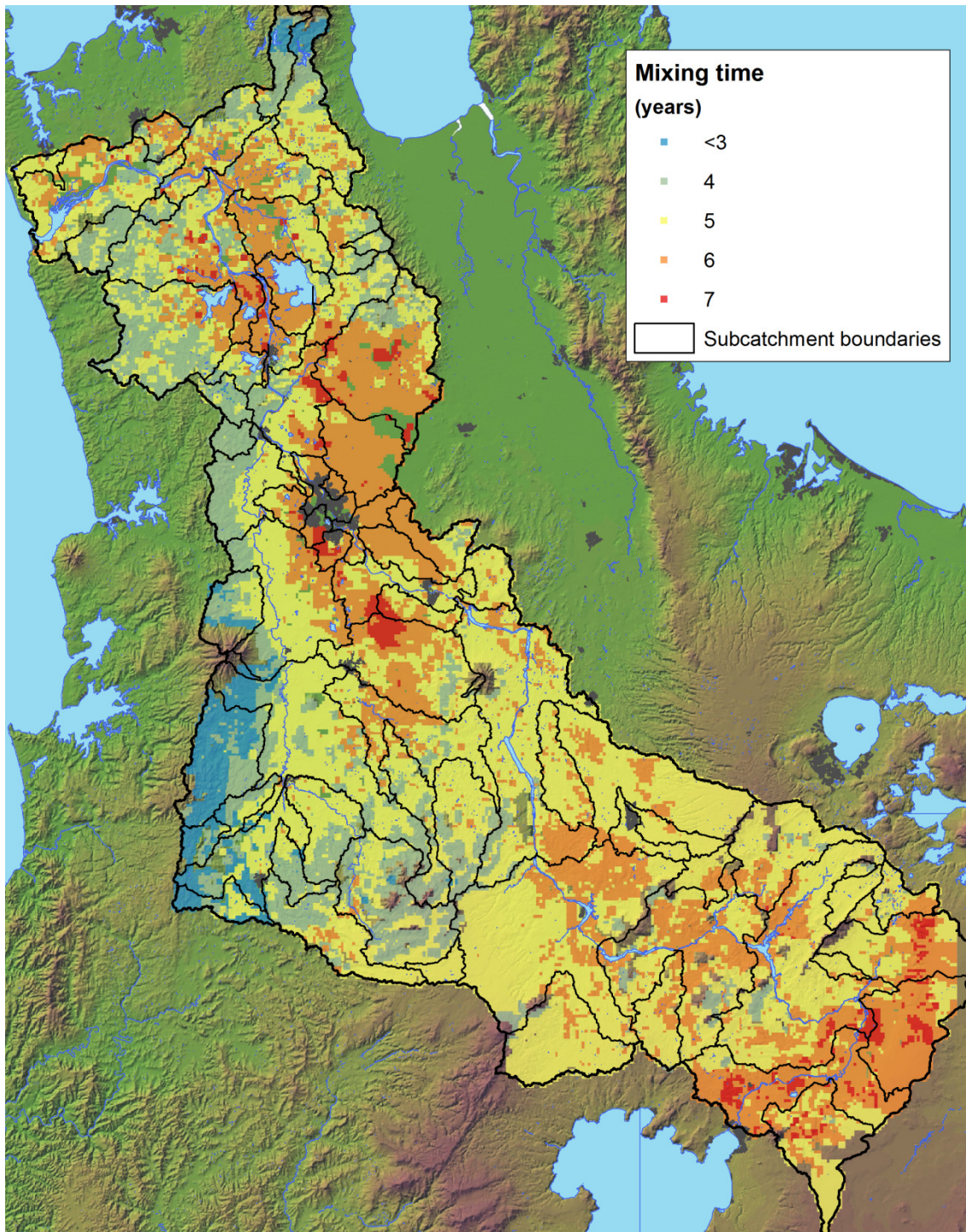


**Figure 14 Estimates of saturated travel time for one year's depth of land surface recharge**

The results of the combined unsaturated and shallow saturated travel time calculations at each 500m grid node are shown in Figure 15. The results of the total travel times are very similar to the unsaturated travel time result, in terms of both magnitude and distribution, with the longer travel times located at higher elevations and short travel times in the low-lying areas.

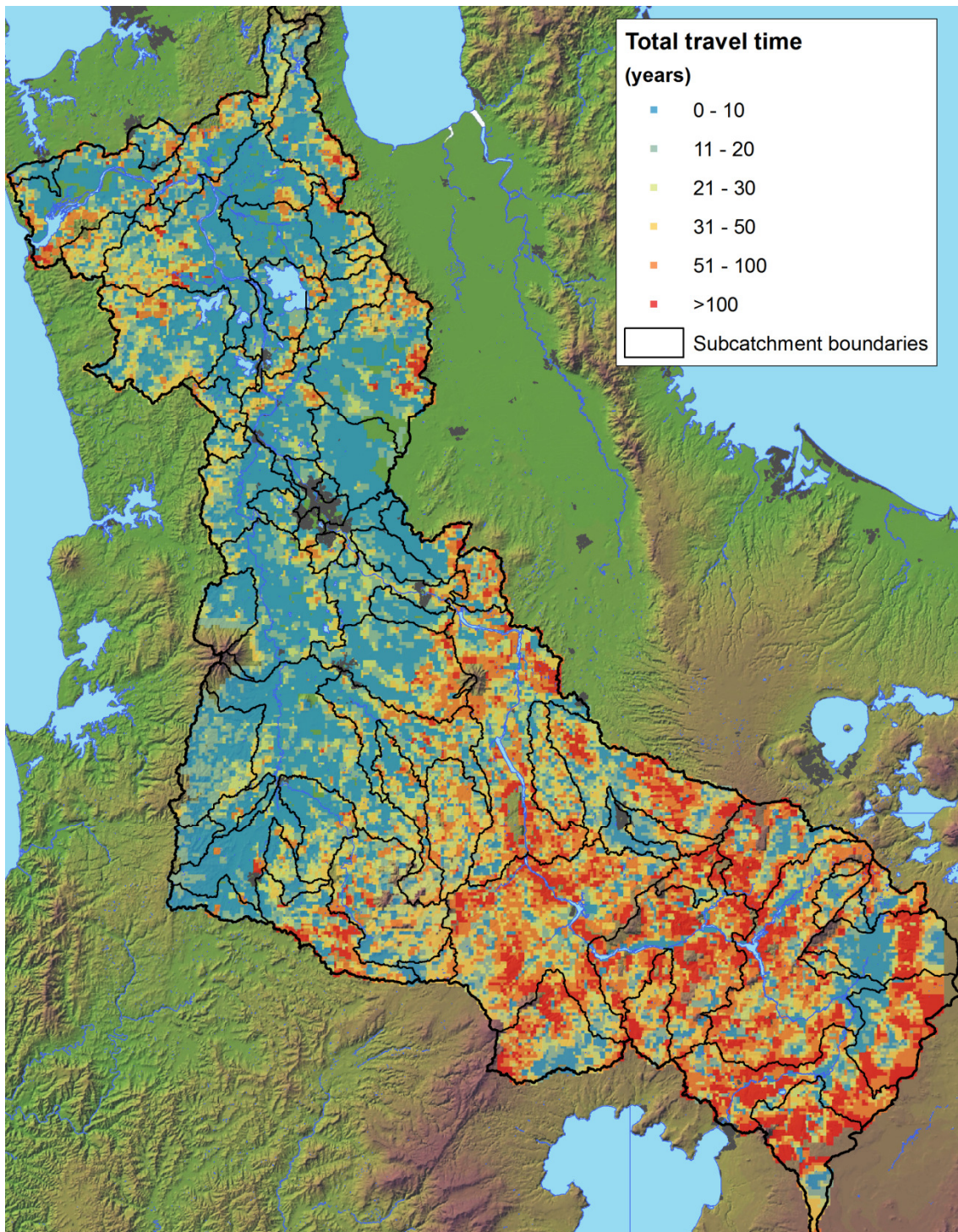


**Figure 15: Predicted total travel times at each grid node**

Travel times are youngest (<10 years) in the lower Waikato basin, the Hamilton basin, and the Waipa basin, i.e. in low-lying parts of the Healthy Rivers catchment with elevations below approx. 100 m. However, rapid travel times are also found at higher elevations along the river and stream valley floors. This is particularly noticeable near Tokoroa and in the Reporoa Basin in spite of elevations of around 300m.

Somewhat greater travel times of 10 to 30 years were predominantly found at higher elevations above 100m, but are also predicted at some lower elevations along the catchment boundaries between streams. The longest time lags are predicted beneath and in the vicinity of volcanoes and ranges, which is a function of a greater depth to the water table in these areas.

There is more uncertainty in the predictions made for hilly terrain because there is considerably less data available to constrain the model, particularly water depth data.

Sub-catchment averages are shown in Figure 16 and are also listed in Appendix 1. Figure 16 also shows the location of shallow tritium samples, which are used for comparative purposes in the next section of this report.

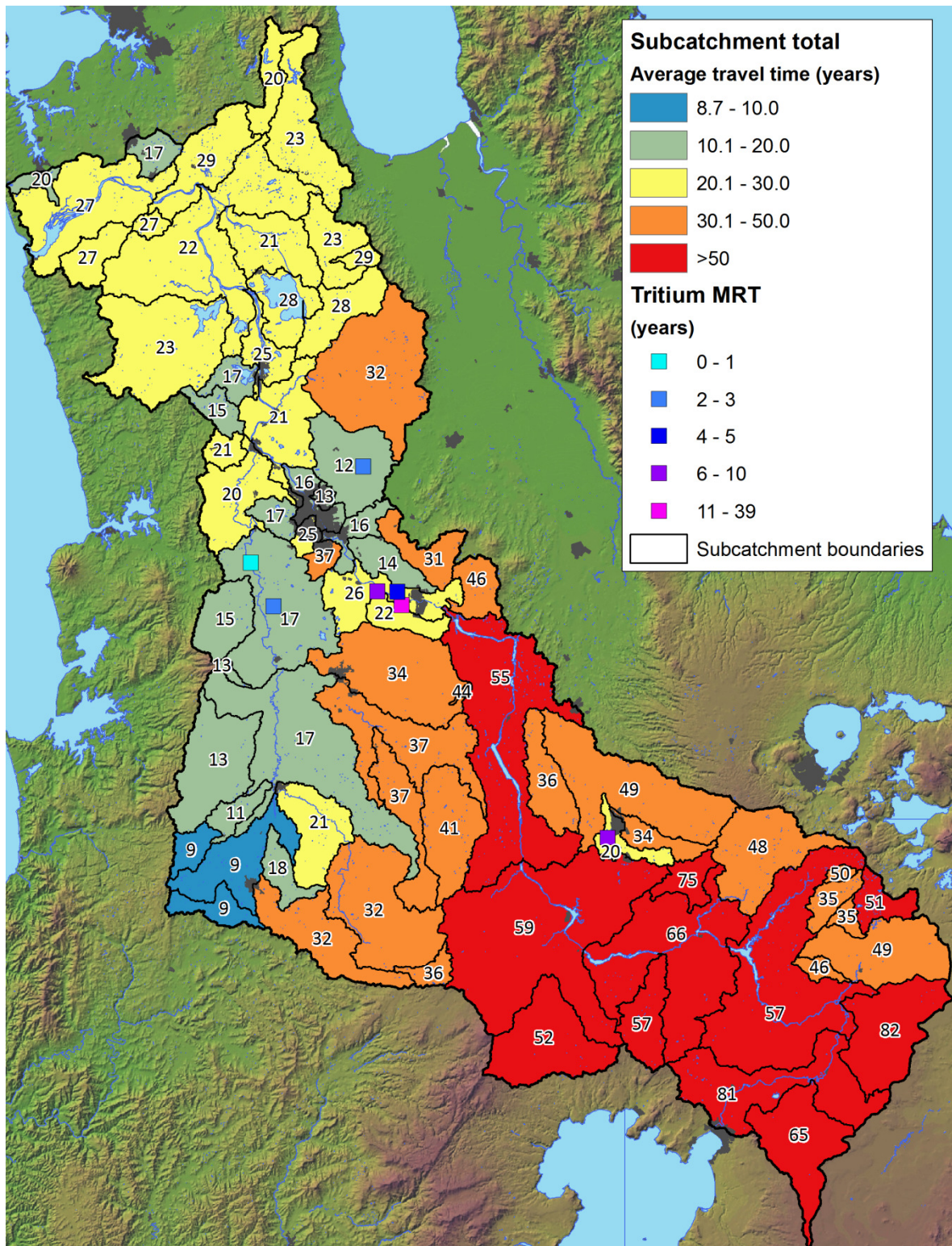


Figure 16: Predicted average total travel time for each sub-catchment



## 5 COMPARISON WITH TRITIUM DATA

The calculation of a saturated penetration time enables a comparison to be made between our modelled predictions and modelled mean residence times based on tritium concentrations measured in groundwater samples. To do this we need to select tritium samples that are of a similar shallow saturated depth. Samples at greater saturated depths have a greater chance of representing multiple recharge sources and are more likely to be influenced by lateral flow paths. We also need to assume that the saturated depth is a fair representation of travel time and that the samples have not been subjected to additional vertical flow gradients.

To select suitable tritium samples to compare with our model results we have calculated an indicative saturated sample depth for each site. The sample depth at each site is assumed to be the bore casing depth minus the groundwater level depth. Scrutiny of the available groundwater tritium data shows that there is a jump in the saturated sample depth from 3m to 13m. The average saturated depth of recharge in our model (recharge divided by porosity) is 1.35m. We have therefore selected tritium sample sites that have a saturated depth of 3m or less. Table 2 shows the sites that we have considered suitable for comparison, together with their mean residence times.

**Table 2: Groundwater tritium data used for comparison with model predictions**

| Bore    | E       | N       | Casing depth (m) | Static water level (mbgl) | Saturated depth (m) | Tritium (years) |
|---------|---------|---------|------------------|---------------------------|---------------------|-----------------|
| 69_173  | 1807942 | 5825285 | 4                | 2.2                       | 1.8                 | 3               |
| 69_81   | 1788964 | 5809114 | 2.3              | 1.2                       | 1                   | 1               |
| 70_22   | 1813640 | 5804238 | 6.42             | 4.18                      | 2.2                 | 5               |
| 70_44   | 1814410 | 5801988 | 18.3             | 16.85                     | 1.5                 | 39              |
| 70_56   | 1810275 | 5804321 | 4.5              | 3.36                      | 1.1                 | 7               |
| 70_65   | 1792806 | 5801812 | 4.3              | 2.12                      | 2.2                 | 2               |
| 72_2373 | 1837740 | 5776550 | 26               | 30                        | 1                   | 8-9 or 41-57    |
| 72_4500 | 1849099 | 5762891 | 6.5              | 13.2                      | 1                   | 5-6 or 41-52    |

Figure 17 shows a comparison between the tritium mean residence times and our mixing model predictions. The tritium samples are not positioned at the centre of our mixing model grid, so we needed to estimate the mixing model predictions at the sample sites. The first method we used was to interpolate values predicted at the model grid nodes to the tritium sample sites. The second approach was to model the travel times at each sample location, with the saturated model depth being determined by the saturated depth shown in Table 2.

The results of our modelling compare well with the reported tritium mean residence times. Note that the mean residence times determined from tritium concentrations do require a mixing model to determine mean residence times. To a large extent, Figure 17 compares the results of two models, although the tritium results are considered to be more reliable since they are constrained by tracer data. The  $r^2$  for the model predictions is 0.75, which means that the lag time model accounts for 75% of the variation in mean residence times.

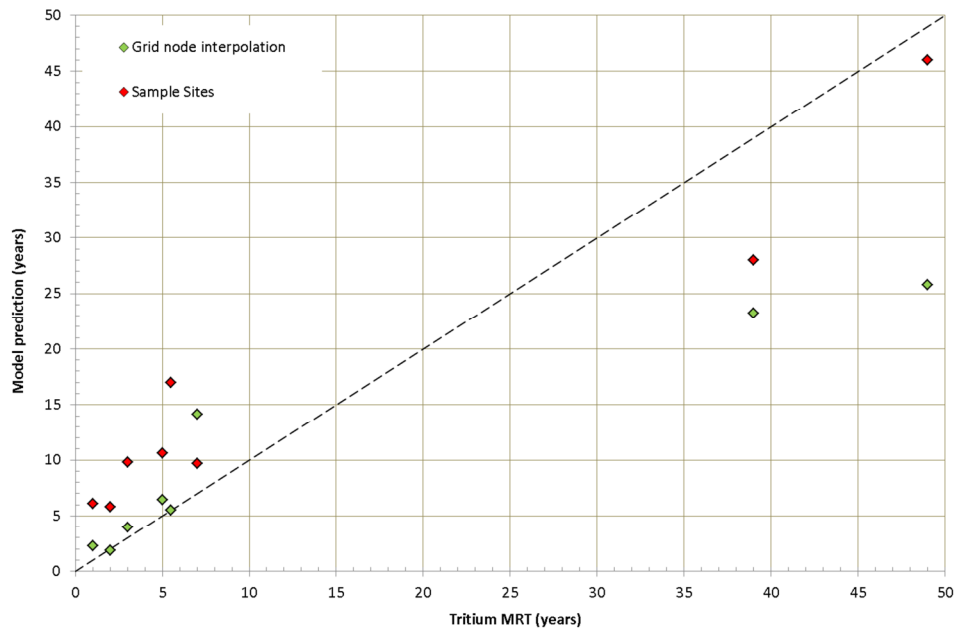


**Figure 17: Comparison between predicted travel times and tritium mean residence time**

## 6 REFERENCES

- Allen, R., Pereira, L.S., Raes, D., Smith, M., 1998. Crop evapotranspiration: guidelines for computing crop water requirements. In: *Irrigation and Drainage Paper 56*. FAO, Rome, 300p.
- Apello, C.A.J. & Postma, D. 2005. *Geochemistry, groundwater and pollution* (2<sup>nd</sup> ed.). Balkema, Rotterdam, 649 p.
- Barkle, G.F., Stenger, R., Wöhling, Th., 2014. Fate of urine nitrogen through a volcanic vadose zone. *Soil Research* 52, 658-670.
- Breuer, L., Eckhardt, K., Frede, H.-G., 2003. Plant parameter values for models in temperate climates. *Ecological Modelling* 169: 237-293.
- Cannavo, P., Richaume, A., & Lafolie, F., 2004. Fate of nitrogen and carbon in the vadose zone: in situ and laboratory measurements of seasonal variations in aerobic respiratory and denitrifying activities. *Soil Biology & Biochemistry* (36), 463–478.
- Close, M., 2010. Critical review of contaminant transport time through the vadose zone. Technical report prepared for Environment Canterbury, Environment Canterbury Report no. R10/113.
- Dagan, G., 1984. Solute transport in heterogeneous porous formations. *Journal of Fluid Mechanics* 145: 151-177.
- Dann R., Close M., Flintoft M., Hector R., Barlow H., Thomas S., Francis G., 2009. Characterization and estimation of hydraulic properties in an alluvial gravel vadose zone. *Vadose Zone Journal* 8: 651–663.
- de Silva, C.S.; and Rushton, K.R. 2007: Groundwater recharge estimation using improved soil moisture balance methodology for a tropical climate with distinct dry seasons. *Hydrological Sciences Journal* 52:5, 1051-1067.
- Domenico, P.A., & Schwartz, F.W., 1998. Physical and chemical hydrogeology (2<sup>nd</sup> ed.). Wiley, New York, 506p.
- Edbrooke, S.W. 2001. Geology of the Auckland area. Institute of Geological & Nuclear Sciences 1:250,000 geological map 3. Lower Hutt, Institute of Geological & Nuclear Sciences. 1 sheet and 75 p. Lower Hutt, New Zealand. Institute of Geological & Nuclear Sciences Limited.
- Edbrooke, S.W. 2005. Geology of the Waikato area. Institute of Geological & Nuclear Sciences 1:250,000 geological map 4. Lower Hutt, Institute of Geological & Nuclear Sciences. 1 sheet and 68 p. Lower Hutt, New Zealand. Institute of Geological & Nuclear Sciences Limited.
- Fetter, C.W., 2001. *Applied Hydrogeology* (4<sup>th</sup> ed.). Prentice Hall, New Jersey.
- Flint, L.E., 2003. Physical and hydraulic properties of volcanic rocks from Yucca Mountain, Nevada. *Water Resources Research* 39 (5) Art. No. 1119.
- Freeze, R.A. & Cherry, J.A., 1979. Groundwater. Prentice Hall, Englewood Cliffs, NJ, 604p.

- Leonard, G.S., Begg, J.G., Wilson, C.J.N., 2010. Geology of the Rotorua area. Institute of Geological & Nuclear Sciences 1:250,000 geological map 5. Lower Hutt, Institute of Geological & Nuclear Sciences. 1 sheet and 102 p. Lower Hutt, New Zealand. Institute of Geological & Nuclear Sciences Limited.
- McLaren, R.G., Cameron, K.C., 1996. Soil science (2<sup>nd</sup> ed.): sustainable production and environmental protection. Oxford University Press, Auckland, 304p.
- McWorter, D.B., & Sunada, D.K., 1977. Groundwater hydrology and hydraulics. Water Resources Publications, Ft. Collins, 290 p.
- Meals, D.W., Dressing, S.A., & Davenport, T.E., 2010. Time lag in water quality response to best management practices: A review. *Journal of Environmental Quality* 39: 85–96.
- NZ Geotechnical Society, 2005. Field Description of Soil and Rock. Guideline for the field classification and description of soil and rock for engineering purposes. NZ Geotechnical Society Inc., Wellington, 38p.
- Rawls, W.J., Ahuja, L.R., Brakensiek, D.L., Shirmohammadi, A., 1992. Infiltration and soil water movement. In: Maidment, D.R. (ed.), 1992. *Handbook of Hydrology*. McGraw-Hill, New York, 1424p.
- Rowe, L., Jackson, R., Fahey, B., 2002. Land use and water resources: Hydrological effects of different vegetation covers. SMF2167: Report No. 5. Report prepared by Landcare Research for Ministry for the Environment.
- Rushton, K.R.; Eilers, V.H.M.; Carter, R.C. 2006: Improved soil moisture balance methodology for recharge estimation. *Journal of Hydrology* 318: 379-399.
- Scotter, D., Heng, L., 2003. Estimating reference crop evapotranspiration in New Zealand. *Journal of Hydrology (NZ)* 42: 1-10.
- Shaap, M.G., Liej, F.J., van Genuchten, M.Th., 1999. A bootstrap-neural network approach to predict soil hydraulic parameters. In: van Genuchten, M.Th., Liej, F.J., Wu, L. (Eds.), *Characterisation and Measurements of the Hydraulic Properties of Unsaturated Porous Media*. University of California, Riverside, CA, USA, 1237-1250.
- Sharpley, A.N., Williams, J.R., 1990. EPIC - Erosion/Productivity Impact Calculator: 1. Model Documentation. US Department of Agriculture Technical Bulletin No. 1768. US Government Printing Office: Washington, DC. 235p.
- Singhal, B.B.S., Gupta, R.P., 2010. Hydrogeology of Volcanic Rocks. In: *Applied Hydrogeology of Fractured Rocks* (2<sup>nd</sup> ed.). Springer Netherlands, 408p.
- Snelder, T., Biggs, B., Weatherhead, M., 2010. New Zealand River Environment Classification User Guide. NIWA Report ME 1026 for Ministry for the Environment, 144p.
- Soil Conservation Service, 1972. *National Engineering Handbook: Section 4, Hydrology*. SCS, US Department of Agriculture.

- Sousa, M.R., Jones, J.P., Frind, E.O., Rudolph, D.L., 2013. A simple method to assess unsaturated zone time lag in the travel time from ground surface to reactor. *Journal of contaminant hydrology* 144, 138-151.
- Stephens, D.B., 1996. *Vadose Zone Hydrology*. CRC Press, Florida, 347p.
- Tschirter, C., Cameron, S., White, P., 2014. Incorporation of hydraulic properties in three-dimensional geological models. *GNS Science Report* 2013/53, 30p.
- Waikato Regional Council, 2015. Contract for Services: Estimation of lag time of water and nitrate flow through the Vadose (Unsaturated) Zone across the Waikato and Waipa River Catchments. Waikato Regional Council Contract No: SAS2014/2015-1099.
- Ward, A. D., Elliot, W. J., 1995. *Environmental Hydrology*. CRC/Lewis Publishers, Boca Raton, Florida, 462p.
- Williams, J.R., 1991. Runoff and Water Erosion. *In: Modelling Plant and Soil Systems, Agronomy Monograph 31*, American Society of Agronomy, Crop Science Society of America, Soil Science Society of America, 439-455.
- Wilson, S.R.; and Lu, X. 2011: Rainfall recharge assessment for Otago groundwater basins. Otago Regional Council technical report, 42p.
- Wöhling, Th., Vrugt, J.A., Barkle, G.F., 2008. Comparison of Three Multiobjective Optimization Algorithms for Inverse Modeling of Vadose Zone Hydraulic Properties. *Soil Science Society of America Journal* 44: 892–898.
- Wyering, L.D., Villeneuve M.C., Wallis I.C., Siratovicha, P.A., Kennedy B.M., Gravley, D.M., Cant, J.L., 2014. Mechanical and physical properties of hydrothermally altered rocks, Taupo Volcanic Zone, New Zealand. *Journal of Volcanology and Geothermal Research* 288: 76-93.

## Appendix 1: Summary of modelling results by sub-catchment

| Catchment                               | Area (m2)   | Depths (mm/year) |          |          |            | Fluxes (m3/s) |          |          | Travel times (years) |                  |             |
|---|-------------|------------------|----------|----------|------------|---------------|----------|----------|----------------------|------------------|-------------|
|   |             | Rain mean        | LSR mean | AET mean | % Recharge | Rain mean     | LSR mean | AET mean | Nodes                | Unsaturated zone | Unsat + sat |
| Awaroa (Rotowaro) at Harris/Te Ohaki Br | 41,278,623  | 1,367            | 301      | 686      | 22         | 1.79          | 0.39     | 0.90     | 132                  | 13.5             | 17.3        |
| Awaroa (Rotowaro) at Sansons Br         | 44,160,409  | 1,514            | 330      | 701      | 21.8       | 2.12          | 0.46     | 0.98     | 145                  | 11.9             | 15.1        |
| Awaroa (Waiuku)                         | 24,704,056  | 1,357            | 266      | 762      | 19.6       | 1.06          | 0.21     | 0.60     | 85                   | 15.2             | 19.6        |
| Firewood                                | 33,722,135  | 1,542            | 355      | 696      | 23         | 1.65          | 0.38     | 0.74     | 112                  | 17.4             | 20.8        |
| Kaniwhaniwha                            | 102,593,485 | 1,976            | 748      | 723      | 37.9       | 6.42          | 2.43     | 2.35     | 251                  | 11.7             | 15.0        |
| Karapiro                                | 67,414,010  | 1,126            | 212      | 677      | 18.8       | 2.41          | 0.45     | 1.45     | 230                  | 41.2             | 45.7        |
| Kawaunui                                | 21,341,460  | 1,520            | 469      | 758      | 30.9       | 1.03          | 0.32     | 0.51     | 73                   | 30.4             | 34.9        |
| Kirikiroa                               | 10,073,011  | 1,132            | 198      | 618      | 17.5       | 0.36          | 0.06     | 0.20     | 39                   | 7.4              | 12.7        |
| Komakorau                               | 163,987,506 | 1,132            | 177      | 627      | 15.6       | 5.88          | 0.92     | 3.26     | 491                  | 7.1              | 12.4        |
| Little Waipa                            | 106,488,691 | 1,434            | 380      | 781      | 26.5       | 4.84          | 1.28     | 2.64     | 399                  | 31.3             | 36.1        |
| Mangaharakeke                           | 54,153,324  | 1,516            | 365      | 733      | 24.1       | 2.60          | 0.63     | 1.26     | 164                  | 70.3             | 75.1        |
| Mangakara                               | 22,349,867  | 1,504            | 457      | 763      | 30.4       | 1.07          | 0.32     | 0.54     | 71                   | 41.1             | 45.6        |
| Mangakino                               | 221,816,238 | 1,551            | 449      | 679      | 28.9       | 10.90         | 3.16     | 4.77     | 740                  | 47.4             | 52.0        |
| Mangakotukutuku                         | 22,841,926  | 1,201            | 153      | 690      | 12.7       | 0.87          | 0.11     | 0.50     | 83                   | 31.4             | 37.1        |
| Mangamingi                              | 46,872,726  | 1,530            | 469      | 776      | 30.7       | 2.27          | 0.70     | 1.15     | 170                  | 15.6             | 20.2        |
| Mangaohoi                               | 4,307,300   | 1,270            | 302      | 499      | 23.8       | 0.17          | 0.04     | 0.07     | 5                    | 39.9             | 44.2        |
| Mangaokewa                              | 172,616,843 | 1,561            | 470      | 689      | 30.1       | 8.54          | 2.57     | 3.77     | 525                  | 28.3             | 32.0        |
| Mangaone                                | 67,229,643  | 1,162            | 243      | 676      | 20.9       | 2.48          | 0.52     | 1.44     | 259                  | 8.7              | 13.8        |
| Mangaonua                               | 80,958,450  | 1,153            | 237      | 636      | 20.6       | 2.96          | 0.61     | 1.63     | 281                  | 26.5             | 31.1        |
| Mangapiko                               | 277,040,992 | 1,187            | 250      | 673      | 21.1       | 10.42         | 2.19     | 5.91     | 935                  | 28.7             | 33.5        |
| Mangapu                                 | 158,190,638 | 1,684            | 536      | 712      | 31.8       | 8.44          | 2.69     | 3.57     | 542                  | 6.4              | 9.0         |
| Mangarama                               | 55,282,371  | 1,707            | 539      | 699      | 31.6       | 2.99          | 0.94     | 1.22     | 175                  | 6.7              | 9.4         |
| Mangarapa                               | 54,429,691  | 1,504            | 409      | 688      | 27.2       | 2.59          | 0.71     | 1.19     | 188                  | 14.5             | 17.7        |
| Mangatangi                              | 193,075,448 | 1,431            | 364      | 670      | 25.4       | 8.76          | 2.23     | 4.10     | 578                  | 19.6             | 23.4        |
| Mangatawhiri                            | 66,714,592  | 1,682            | 523      | 670      | 31.1       | 3.56          | 1.11     | 1.42     | 149                  | 17.0             | 20.3        |
| Mangatutu                               | 122,690,529 | 1,526            | 487      | 688      | 31.9       | 5.93          | 1.89     | 2.67     | 375                  | 32.8             | 36.9        |
| Mangauika                               | 9,781,272   | 2,338            | 909      | 633      | 38.9       | 0.72          | 0.28     | 0.20     | 11                   | 10.1             | 12.8        |

| Catchment                     | Area (m2)   | Depths (mm/year) |          |          |            | Fluxes (m3/s) |          |          | Travel times (years) |                  |             |
|-------------------------------|-------------|------------------|----------|----------|------------|---------------|----------|----------|----------------------|------------------|-------------|
|                               |             | Rain mean        | LSR mean | AET mean | % Recharge | Rain mean     | LSR mean | AET mean | Nodes                | Unsaturated zone | Unsat + sat |
| Mangawara                     | 358,835,188 | 1,147            | 192      | 625      | 16.7       | 13.04         | 2.18     | 7.11     | 998                  | 27.0             | 31.6        |
| Mangawhero                    | 53,472,492  | 1,171            | 212      | 677      | 18.1       | 1.98          | 0.36     | 1.15     | 189                  | 16.8             | 21.9        |
| Matahuru                      | 106,285,637 | 1,243            | 281      | 611      | 22.6       | 4.19          | 0.95     | 2.06     | 315                  | 24.2             | 28.3        |
| Moakurua                      | 206,299,004 | 1,994            | 785      | 692      | 39.4       | 13.04         | 5.13     | 4.52     | 608                  | 10.1             | 13.0        |
| Ohaeroa                       | 20,325,799  | 1,357            | 269      | 739      | 19.8       | 0.87          | 0.17     | 0.48     | 68                   | 23.0             | 26.9        |
| Ohote                         | 39,943,852  | 1,316            | 271      | 653      | 20.6       | 1.67          | 0.34     | 0.83     | 125                  | 12.2             | 17.2        |
| Opuatia                       | 70,670,605  | 1,471            | 294      | 708      | 20         | 3.29          | 0.66     | 1.59     | 244                  | 23.6             | 27.4        |
| Otamakokore                   | 45,727,344  | 1,519            | 482      | 754      | 31.7       | 2.20          | 0.70     | 1.09     | 146                  | 30.4             | 34.9        |
| Pokaiwhenua                   | 327,010,581 | 1,499            | 401      | 762      | 26.8       | 15.53         | 4.16     | 7.90     | 1221                 | 44.0             | 48.7        |
| Pueto                         | 200,229,389 | 1,302            | 345      | 659      | 26.5       | 8.26          | 2.19     | 4.18     | 561                  | 60.6             | 65.4        |
| Puniu at Bartons Corner Rd Br | 226,526,740 | 1,307            | 364      | 714      | 27.9       | 9.38          | 2.61     | 5.13     | 839                  | 32.1             | 36.8        |
| Puniu at Wharepapa            | 168,525,739 | 1,562            | 513      | 728      | 32.8       | 8.34          | 2.74     | 3.89     | 579                  | 36.7             | 40.9        |
| Tahunaatara                   | 207,320,709 | 1,497            | 418      | 737      | 27.9       | 9.83          | 2.75     | 4.84     | 621                  | 43.3             | 47.8        |
| Torepatutahi                  | 216,787,201 | 1,174            | 250      | 614      | 21.3       | 8.06          | 1.72     | 4.22     | 736                  | 76.7             | 82.0        |
| Waerenga                      | 19,592,552  | 1,268            | 321      | 610      | 25.3       | 0.79          | 0.20     | 0.38     | 57                   | 25.0             | 28.8        |
| Waikare                       | 69,986,830  | 1,133            | 194      | 595      | 17.1       | 2.51          | 0.43     | 1.32     | 234                  | 23.2             | 27.9        |
| Waikato at Bridge St Br       | 42,304,185  | 1,151            | 225      | 642      | 19.5       | 1.54          | 0.30     | 0.86     | 162                  | 10.7             | 15.9        |
| Waikato at Horotiu Br         | 31,481,182  | 1,186            | 230      | 622      | 19.4       | 1.18          | 0.23     | 0.62     | 104                  | 11.2             | 16.4        |
| Waikato at Huntly-Tainui Br   | 167,657,863 | 1,281            | 259      | 648      | 20.2       | 6.81          | 1.38     | 3.44     | 544                  | 16.6             | 20.9        |
| Waikato at Karapiro           | 520,785,814 | 1,379            | 368      | 723      | 26.7       | 22.76         | 6.07     | 11.93    | 1735                 | 50.1             | 54.7        |
| Waikato at Mercer Br          | 438,350,295 | 1,257            | 220      | 664      | 17.5       | 17.46         | 3.06     | 9.22     | 1432                 | 18.1             | 22.3        |
| Waikato at Narrows            | 121,759,930 | 1,184            | 230      | 659      | 19.4       | 4.57          | 0.89     | 2.54     | 456                  | 21.3             | 26.3        |
| Waikato at Ohaaki             | 286,290,582 | 1,220            | 262      | 677      | 21.5       | 11.07         | 2.38     | 6.14     | 1018                 | 75.4             | 80.6        |
| Waikato at Ohakuri            | 518,576,894 | 1,401            | 376      | 745      | 26.8       | 23.02         | 6.18     | 12.24    | 1709                 | 52.0             | 56.8        |
| Waikato at Port Waikato       | 259,489,366 | 1,376            | 260      | 708      | 18.9       | 11.31         | 2.14     | 5.82     | 679                  | 22.3             | 26.6        |
| Waikato at Rangiriri          | 57,422,954  | 1,155            | 210      | 579      | 18.2       | 2.10          | 0.38     | 1.05     | 193                  | 20.7             | 25.2        |
| Waikato at Tuakau Br          | 148,970,142 | 1,295            | 224      | 645      | 17.3       | 6.11          | 1.06     | 3.04     | 411                  | 24.2             | 28.5        |
| Waikato at Waipapa            | 683,617,850 | 1,545            | 419      | 715      | 27.1       | 33.47         | 9.08     | 15.49    | 2342                 | 54.0             | 58.7        |
| Waikato at Whakamaru          | 437,727,930 | 1,407            | 322      | 704      | 22.9       | 19.52         | 4.47     | 9.77     | 1237                 | 61.6             | 66.3        |

| Catchment                        | Area (m2)   | Depths (mm/year) |          |          |            | Fluxes (m3/s) |          |          | Travel times (years) |                  |             |
|----------------------------------|-------------|------------------|----------|----------|------------|---------------|----------|----------|----------------------|------------------|-------------|
|                                  |             | Rain mean        | LSR mean | AET mean | % Recharge | Rain mean     | LSR mean | AET mean | Nodes                | Unsaturated zone | Unsat + sat |
| Waiotapu at Campbell             | 60,152,295  | 1,419            | 371      | 690      | 26.1       | 2.70          | 0.71     | 1.32     | 201                  | 46.2             | 50.8        |
| Waiotapu at Homestead            | 204,537,413 | 1,314            | 321      | 629      | 24.4       | 8.52          | 2.08     | 4.08     | 594                  | 44.3             | 49.2        |
| Waipa at Mangaokewa Rd           | 32,142,964  | 1,624            | 507      | 673      | 31.2       | 1.65          | 0.52     | 0.69     | 120                  | 31.5             | 36.0        |
| Waipa at Otewa                   | 286,654,261 | 1,639            | 560      | 662      | 34.2       | 14.89         | 5.09     | 6.01     | 765                  | 28.0             | 31.8        |
| Waipa at Otorohanga              | 136,519,059 | 1,459            | 421      | 711      | 28.9       | 6.31          | 1.82     | 3.08     | 453                  | 17.5             | 21.4        |
| Waipa at Pirongia-Ngutunui Rd Br | 434,617,188 | 1,534            | 503      | 708      | 32.8       | 21.13         | 6.93     | 9.75     | 1418                 | 13.0             | 16.6        |
| Waipa at SH23 Br Whatawhata      | 315,059,784 | 1,497            | 412      | 718      | 27.5       | 14.95         | 4.11     | 7.17     | 981                  | 12.9             | 17.0        |
| Waipa at Wainaro Rd Br           | 153,162,646 | 1,523            | 367      | 706      | 24.1       | 7.39          | 1.78     | 3.43     | 528                  | 16.4             | 20.3        |
| Waipapa                          | 100,485,321 | 1,437            | 394      | 708      | 27.4       | 4.58          | 1.25     | 2.25     | 369                  | 52.5             | 57.2        |
| Waitawhiriwhiri                  | 11,107,152  | 1,219            | 136      | 693      | 11.2       | 0.43          | 0.05     | 0.24     | 35                   | 19.1             | 24.9        |
| Waitomo at SH31 Otorohanga       | 43,928,758  | 1,662            | 486      | 705      | 29.2       | 2.31          | 0.68     | 0.98     | 137                  | 8.5              | 11.3        |
| Waitomo at Tumutumu Rd           | 43,177,609  | 2,006            | 782      | 708      | 39         | 2.74          | 1.07     | 0.97     | 141                  | 6.4              | 8.7         |
| Whakapipi                        | 44,820,443  | 1,310            | 224      | 764      | 17.1       | 1.86          | 0.32     | 1.09     | 149                  | 13.1             | 17.4        |
| Whakauru                         | 52,236,471  | 1,543            | 472      | 768      | 30.6       | 2.55          | 0.78     | 1.27     | 193                  | 29.2             | 33.8        |
| Whangamarino at Island Block Rd  | 143,647,592 | 1,161            | 210      | 612      | 18.1       | 5.28          | 0.96     | 2.79     | 396                  | 16.2             | 20.7        |
| Whangamarino at Jefferies Rd Br  | 97,011,860  | 1,201            | 250      | 621      | 20.8       | 3.69          | 0.77     | 1.91     | 310                  | 18.8             | 23.0        |
| Whangape                         | 306,244,362 | 1,392            | 275      | 697      | 19.8       | 13.51         | 2.67     | 6.76     | 1078                 | 19.3             | 23.2        |
| Whirinaki                        | 10,796,254  | 1,527            | 493      | 747      | 32.3       | 0.52          | 0.17     | 0.26     | 29                   | 45.4             | 49.6        |



## Appendix 2: Hydraulic parameter values derived from texture

| Main Rock         | Hardness | Equivalent Texture | Porosity | $\alpha$ | $\eta$ |
|-------------------|----------|--------------------|----------|----------|--------|
| Andesite          | Hard     | Clayey silt        | 0.15     | 1.58     | 1.42   |
| Andesite          | Firm     | Clayey silt        | 0.17     | 1.58     | 1.42   |
| Basalt            | Hard     | Clayey silt        | 0.12     | 1.58     | 1.42   |
| Basalt            | Firm     | Clayey silt        | 0.13     | 1.58     | 1.42   |
| Basaltic andesite | Hard     | Clayey silt        | 0.14     | 1.58     | 1.42   |
| Basaltic andesite | Firm     | Clayey silt        | 0.15     | 1.58     | 1.42   |
| Breccia           | Soft     | Gravel             | 0.15     | 493      | 2.19   |
| Breccia           | Firm     | Clayey sand        | 0.1      | 3.48     | 1.75   |
| Chert             | Hard     | Glassey            | NA       | NA       | NA     |
| Clay              | Hard     | Clay               | 0.47     | 1.49     | 1.25   |
| Clay              | Firm     | Clay               | 0.47     | 1.49     | 1.25   |
| Clay              | Soft     | Clay               | 0.47     | 1.49     | 1.25   |
| Conglomerate      | Soft     | Gravel             | 0.28     | 493      | 2.19   |
| Conglomerate      | Firm     | Clayey sand        | 0.25     | 3.48     | 1.75   |
| Dacite            | Hard     | Silty clay         | 0.18     | 1.62     | 1.32   |
| Dacite            | Firm     | Silty clay         | 0.2      | 1.62     | 1.32   |
| Fill              | Soft     | Silty sand         | 0.37     | 3.48     | 1.75   |
| Fill              | Firm     | Clayey sand        | 0.4      | 3.48     | 1.75   |
| Gravel            | Soft     | Gravel             | 0.28     | 493      | 2.19   |
| Greywacke         | Hard     | Clayey sand        | 0.15     | 3.48     | 1.75   |
| Ignimbrite        | Soft     | Clayey silt        | 0.45     | 1.58     | 1.42   |
| Ignimbrite        | Firm     | Silty clay         | 0.45     | 1.62     | 1.32   |
| Limestone         | Hard     | Fine sand          | 0.12     | 2.51     | 3.55   |
| Limestone         | Firm     | Silty sand         | 0.15     | 3.48     | 1.75   |
| Mud               | Soft     | Clay               | 0.47     | 1.49     | 1.25   |
| Mudstone          | Hard     | Clay               | 0.05     | 1.49     | 1.25   |
| Olivine basalt    | Hard     | Clayey silt        | 0.1      | 1.58     | 1.42   |
| Olivine basalt    | Firm     | Clayey silt        | 0.11     | 1.58     | 1.42   |
| Peat              | Soft     | Clay               | 0.4      | 1.49     | 1.25   |
| Pumice            | Soft     | Coarse sand        | 0.6      | 29.4     | 3.28   |
| Rhyolite          | Hard     | Clayey silt        | 0.18     | 1.58     | 1.42   |
| Rhyolite          | Firm     | Clayey silt        | 0.2      | 1.58     | 1.42   |
| Sand              | Soft     | Medium sand        | 0.36     | 3.52     | 3.18   |
| Sandstone         | Soft     | Medium sand        | 0.25     | 3.52     | 3.18   |
| Sandstone         | Firm     | Fine sand          | 0.2      | 2.51     | 3.55   |
| Sandstone         | Hard     | Silty sand         | 0.15     | 3.48     | 1.75   |
| Silt              | Soft     | Silt               | 0.43     | 0.66     | 1.68   |
| Siltstone         | Hard     | Clayey silt        | 0.12     | 1.58     | 1.42   |
| Tephra            | Firm     | Silty sand         | 0.37     | 3.48     | 1.75   |
| Tuff              | Soft     | Fine sand          | 0.38     | 2.51     | 3.55   |
| Tuff              | Firm     | Clayey sand        | 0.4      | 3.48     | 1.75   |
| Turbidite         | Hard     | Clayey silt        | 0.1      | 1.58     | 1.42   |

**Key:** *Main Rock* = Q-Map main lithology classification, *Hardness* = an estimate of the lithology hardness, *Equivalent texture* = equivalent clastic texture given to volcanic lithologies, *Porosity* = effective porosity,  $\alpha$  = Van Genuchten parameter for inverse air-entry pressure,  $\eta$  = Genuchten parameter for pore size distribution